

Chemistry of Iridium(I) Cyclooctadiene Compounds with Thiapentadienyl, Sulfinylpentadienyl, and Butadienesulfonyl Ligands

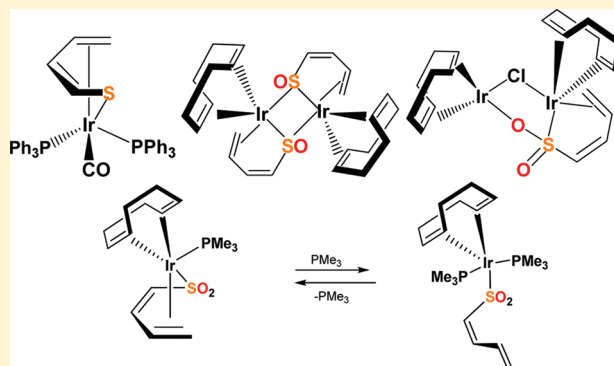
Procoro Gamero-Melo,[†] Patricia Andrea Melo-Trejo, Marisol Cervantes-Vasquez, Nelly Paola Mendizabal-Navarro, Brenda Paz-Michel, Tere Isabel Villar-Masetto, Miguel Angel Gonzalez-Fuentes, and M. Angeles Paz-Sandoval*

Departamento de Química, Centro de Investigación y de Estudios Avanzados del IPN, Avenida IPN # 2508, San Pedro Zacatenco, México 07360, D.F., México

[†]Centro de Investigación y de Estudios Avanzados del IPN, Unidad Saltillo, Carretera Saltillo-Monterrey Km 13.5, C.P. 25900, Ramos Arizpe, Coahuila, Mexico

S Supporting Information

ABSTRACT: The metathesis reaction of $[(\eta^4\text{-COD})\text{Ir}(\mu\text{-Cl})_2]$ (**4**) with two equivalents of the sodium thiapentadienide (**1Na**) or potassium sulfinylpentadienide salt (**2K**) led to the formation of the corresponding dimers $[(\eta^4\text{-COD})\text{Ir}(\mu_2\text{-}1\text{-}2,5\text{-}\eta\text{-CH}_2\text{CHCHCHS})_2]$ (**5**) and $[(\eta^4\text{-COD})\text{Ir}(\mu_2\text{-}1\text{-}2,5\text{-}\eta\text{-CH}_2\text{CHCHCHSO})_2]$ (**9**). The single-crystal analysis of **5** and **9** reveals the presence of the thiapentadienyl or sulfinylpentadienyl ligands bridging through the sulfur atoms and the terminal double bonds to both iridium centers. Treatment of **5** with two equivalents of PMe_3 produces $[(\eta^4\text{-COD})\text{Ir}(1\text{-}2,5\text{-}\eta\text{-CH}_2\text{CHCHCHS})\text{PMe}_3]$ (**6**), while compound $\text{Ir}(1\text{-}2,5\text{-}\eta\text{-CH}_2\text{CHCHCHS})(\text{CO})(\text{PPh}_3)_2$ (**8**) is obtained from reaction of $\text{Ir}(\text{CO})(\text{Cl})(\text{PPh}_3)_2$ (**7**) with potassium thiapentadienide (**1K**). The ^1H and ^{13}C NMR support the preferred U conformation and the same $\eta^{2,1}$ -bonding mode of the thiapentadienyl ligand in each case. The reaction of **4** with butadienesulfinate salts $\text{M}[\text{CH}_2\text{CHCHCHSO}_2]$ (**3M**) ($\text{M} = \text{Li}, \text{K}$) affords the ion-pair complexes $[(\eta^4\text{-COD})\text{IrCl}(1\text{-}2,5\text{-}\eta\text{-CH}_2\text{CHCHCHS}(\text{O}_2\text{-M}^+))]$ ($\text{M} = \text{Li}, \text{10}; \text{M} = \text{K}, \text{11}$). Compound $(\eta^4\text{-COD})\text{Ir}(\mu\text{-Cl})(1\text{-}2\text{-}\eta\text{-S,O-}\mu\text{-OSOCHCHCHCH}_2)\text{Ir}(\eta^4\text{-COD})$ (**12**) can be isolated if the reaction of **4** with **3K** is carried out at low temperature and after a short period of time in solution. The crystal structure of **12** shows a dinuclear compound where the butadienesulfonyl is bridging through the S and one of the O atoms to the iridium center. In solution, **12** dissociates in the presence of coordinating solvents, such as $\text{DMSO-}d_6$ or $\text{THF-}d_8$, while the dinuclear asymmetric structure of **12** remains in CDCl_3 . The series of pentacoordinated $\text{Ir}(\text{I})$ complexes of general formula $[(\eta^4\text{-COD})\text{Ir}(1\text{-}2,5\text{-}\eta\text{-CH}_2\text{CHCHCHSO}_2)\text{L}]$ ($\text{L} = \text{PMe}_3, \text{14}; \text{PMe}_2\text{Ph}, \text{15}; \text{PMePh}_2, \text{16}; \text{PPh}_3, \text{17}; \text{DMSO}, \text{18}; \text{and CO}, \text{19}$) can be obtained, under mild conditions, from **11** and the corresponding ligand **L**, which shows different σ or π donor–acceptor properties. The substituted phosphine derivative $[(\eta^4\text{-COD})\text{Ir}(5\text{-}\eta\text{-CH}_2\text{CHCHCHSO}_2)(\text{PMe}_3)_2]$ (**20**) can be prepared directly from **14** and an excess of PMe_3 . A comparative study of these derivatives was carried out through the analysis of the IR, mass spectrometry, and ^1H , ^{13}C , and ^{31}P NMR spectroscopy, as well as through the crystalline structures of **12**, **14**, **15**, and **17–20**, and allowed establishing trends among them. The presence of the butadienesulfonyl ligand in complexes **14–19** induces a total asymmetry that is reflected through the ^1H and ^{13}C NMR. The preferred coordination mode (1-2,5- η -) in the butadienesulfonyl ligand for complexes **14–19** was confirmed. A better synthetic procedure for **14** is described if $[(\eta^4\text{-COD})\text{IrClPMe}_3]$ (**21**) reacts with **3K**. In contrast, no synthetic advantage was found in the formation of **17** or **20** when $[(\eta^4\text{-COD})\text{IrClPPh}_3]$ (**22**) or $[(\eta^4\text{-COD})\text{IrCl}(\text{PMe}_3)_2]$ (**23**) is used as a precursor. Monitoring reactions through ^1H and ^{31}P NMR of **11**, **12**, and **14** in the presence of PMe_3 and **23** with **3K** afforded mixtures of compounds, from which an equilibrium in the reaction mixture is proposed.



INTRODUCTION

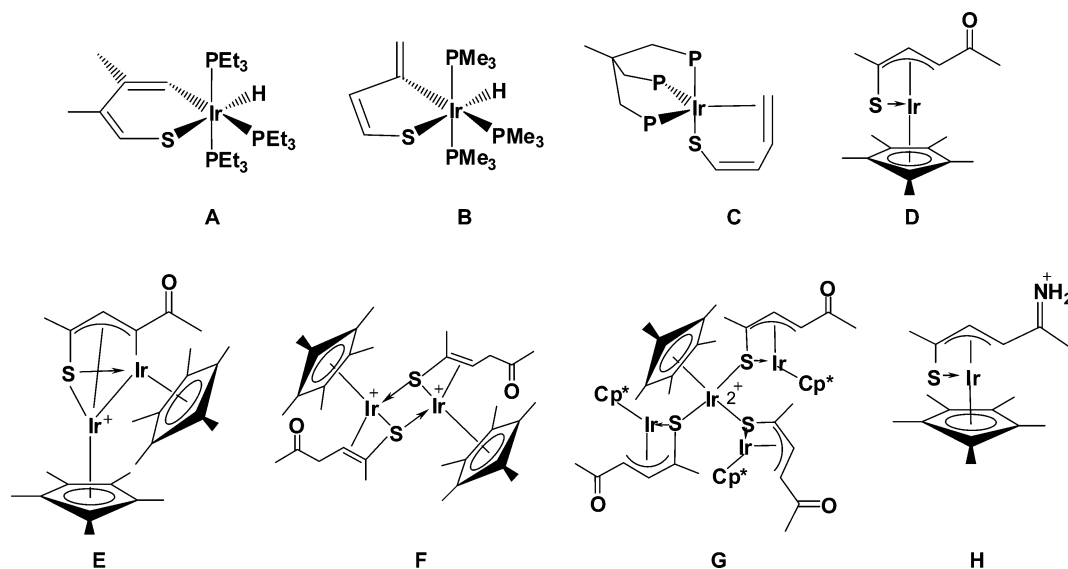
The presence of the sulfur atom in heterodienyl ligands has shown an interesting and versatile chemistry, as can be appreciated comparatively from the results obtained with previous analogous pentadienyl complexes.¹ Since 1992, there has been an interest in the reactions between iridium and acyclic thiapentadienyl ligands because of the range of

coordination modes that are adopted by this ligand and the possibility of rearrangements observed. The electron-rich complexes $\text{IrCl}(\text{PR}_3)_3$ ($\text{R} = \text{Me}, \text{Et}$)² is an example of this versatility; its reactivity, with the thiapentadienide, is quite

Received: August 2, 2011

Published: December 27, 2011

Chart 1



different depending on the substituent R, which affords interesting molecules derived from intramolecular C–H bond activation. These reactions generate iridathiacyclohexadiene^{2–4} and iridathiacyclopentene,^{2–5} where the former six-membered-ring compound can gradually convert to the corresponding iridathiacycle with an exocyclic double bond, such as examples A and B in Chart 1. Also, iridathiabenzene molecules have been obtained using acyclic thiapentadienide salts as precursors.^{3,6}

The chemistry of the thiapentadienyl compounds with transition metals has also been developed, since 1987, based on thiophenes, which, once coordinated with transition metals, result in the activation of the heterocycle due to nucleophilic attack by a variety of anions, including hydride donors,^{7–9} or from electrophilic addition.¹⁰

These interactions between metals and thiophenes have been the subject of much study because of their relevance to the understanding of the chemistry of hydrodesulfurization. In particular, this ring-opening reaction of thiophene with iridium has been observed when $\text{Ir}(\text{H})_2(\text{triphos})(\text{Et})$ produces, by reductive elimination of ethane, the reactive 16-electron fragment $(\text{triphos})\text{IrH}$ [$\text{triphos} = \text{MeC}(\text{CH}_2\text{PPh}_2)_3$], which affords the thiapentadienyl ligand coordinated through the terminal double bond and the sulfur to iridium in $\text{Ir}(1\text{-}2,5\text{-}\eta\text{-CH}_2\text{CHCHCHS})(\text{triphos})$ (C).¹¹

Reactions of aqueous base with the dicationic iridium thiophene complex $[\text{Cp}^*\text{Ir}(2,5\text{-dimethyl-}\eta^5\text{-thiophene})][\text{X}]_2$ ($\text{X} = \text{BF}_4, \text{OTf}$) afford a mixture of mono-, di-, and tetranuclear compounds $[\text{Cp}^*\text{Ir}(\eta^4\text{-SC}(\text{Me})\text{CHCHC}(\text{O})\text{Me})]$ (D), $[(\text{Cp}^*\text{Ir})_2(\mu_2, \eta^4\text{-SC}(\text{Me})\text{CHCHC}(\text{O})\text{Me})](\text{BF}_4)$ (E), $[\text{Cp}^*\text{Ir}(\mu_2, \eta^3\text{-SC}(\text{Me})\text{CHCH}_2\text{C}(\text{O})\text{Me})_2](\text{BF}_4)_2$ (F), and $(\text{Cp}^*\text{Ir})_3[\text{Cp}^*\text{Ir}(\eta^4\text{-SC}(\text{Me})\text{CHCHC}(\text{O})\text{Me})]_3(\text{BF}_4)_2$ (G).¹² The mononuclear acylthiolate complex $[\text{Cp}^*\text{Ir}(\eta^4\text{-SC}(\text{Me})\text{-CHCHC}(\text{O})\text{Me})]$ (D) was also reported from the reaction of $[\text{Cp}^*\text{Ir}(2,5\text{-dimethyl-}\eta^5\text{-thiophene})][\text{BF}_4]_2$ with PhLi in THF or $(n\text{-Bu})_4\text{N}^+\text{OH}^-$ in MeCN,¹³ and the dicationic thiophene complex readily adds secondary amines to afford $[\text{Cp}^*\text{Ir}(\eta^4\text{-SC}(\text{Me})\text{CHCHC}(\text{Me})(\text{N}(\text{CH}_2)_n)](\text{BF}_4)$ ($n = 4, 5$) (H).¹⁴

Alternative methods for the synthesis of the corresponding oxidative derivatives of the thiapentadienyl ligand, such as the 5-oxothiapentadienyl or sulfinylpentadienyl, and 5,5-dioxothia-

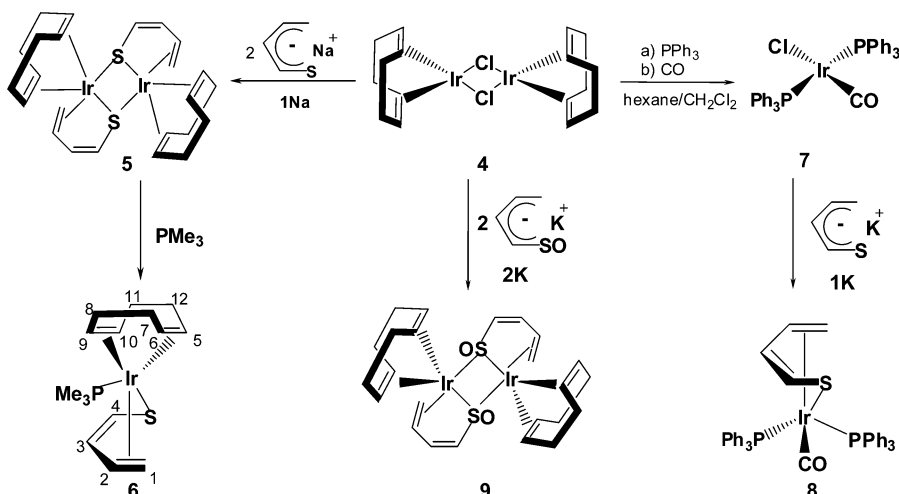
pentadienyl or butadienesulfonyl, have been developed in the past decade, and, consequently, their capability as ligands in organometallic transition compounds is still unknown.

Particularly, only a couple of examples in iridium chemistry have been reported related with the metathesis reaction of $[\text{Cp}^*\text{IrCl}_2]_2$ with butadienesulfinate salts. Previous studies show that $[\text{Cp}^*\text{IrCl}_2]_2$, according to the size of the cation in $\text{M}[\text{CH}_2\text{CHCHCHSO}_2]$ ($\text{M} = \text{Li}, 3\text{Li}; \text{M} = \text{K}, 3\text{K}$), yields dinuclear $[\text{Cp}^*\text{Ir}(\text{Cl})_2\{(\text{S-}\eta\text{-CH}_2\text{CHCHCHSO}_2)\}(\text{Li})(\text{THF})_2]$ or mononuclear $[\text{Cp}^*\text{IrCl}(1\text{-}2,5\text{-}\eta\text{-CH}_2\text{CHCHCHSO}_2)]$ compounds, respectively.¹⁵ A strong dependence of reaction efficiency on the nature of the phosphine has been observed in $\text{Cp}^*\text{IrCl}(\text{S-}\eta\text{-CH}_2\text{CHCHCHSO}_2)\text{PR}_3$, ($\text{R} = \text{Me}, \text{Ph}$) from addition reaction of $\text{Cp}^*\text{IrCl}[1\text{-}2,5\text{-}\eta\text{-CH}_2\text{CHCHCHSO}_2]$ with PR_3 ($\text{R} = \text{Me}, \text{Ph}$) or through the metathesis reaction of $\text{Cp}^*\text{Ir}(\text{Cl})_2\text{PR}_3$ with the potassium butadienesulfinate.¹⁶

The butadienesulfonyl ligand has shown different coordination modes, chemical versatility, and stability, as observed by its isomerization^{16–18} and inter- and intramolecular hydrogen interactions.^{18,19}

The chemistry of iridium with the cyclooctadiene ligand is now explored; the first examples of dimeric structures $[(\eta^4\text{-COD})\text{Ir}(\mu_2\text{-}1\text{-}2,5\text{-}\eta\text{-CH}_2\text{CHCHCHE})]_2$ ^{17,20} ($\text{E} = \text{S}, \text{SO}$), which include bridging thia- and sulfinyl-pentadienyl ligands,¹⁹ were obtained after treatment of $[(\eta^4\text{-COD})\text{Ir}(\mu\text{-Cl})]_2$ with sodium thiapentadienide and potassium sulfinyl-pentadienide. The reaction of lithium and potassium butadienesulfinate with $[(\eta^4\text{-COD})\text{Ir}(\mu\text{-Cl})]_2$ produced the corresponding ion-pair complexes $(\eta^4\text{-COD})\text{IrCl}(\text{dioxo-thiapentadienide})$. Representative examples of the $(\eta^4\text{-COD})\text{Ir}(\text{dioxo-thiapentadienyl})\text{L}$ compounds with two-electron-donor ligands L were synthesized, including derivatives with a σ -donor (DMSO), a π -acceptor (CO), and also different phosphines, which smoothly change their steric and electronic properties, and a corresponding comparative study was established. The interesting chemistry displayed by these oxygen-containing thiapentadienyl molecules, and especially their major differences relative to the simple thiapentadienyl complexes, suggests that the sulfinyl-pentadienyl and dioxo-thiapentadienyl ligands should also prove interesting to study.

Scheme 1



RESULTS AND DISCUSSION

A. Thiapentadienyl Chemistry. Reaction of $[(\eta^4\text{-COD})\text{Ir}(\mu\text{-Cl})_2]$ (**4**) with two equivalents of sodium thiapentadienide (**1Na**), prepared *in situ* in $\text{DMSO-}d_6$, led to the formation of the dimer $[(\eta^4\text{-COD})\text{Ir}(\mu_2\text{-1-2,5-}\eta\text{-CH}_2\text{CHCHCHS})_2]$ (**5**)^{17,20} in 47% yield (Scheme 1).

The X-ray crystal structure contains two iridium atoms, two thiapentadienyl ligands, and two cyclooctadiene ligands, Figure 1. Crystal data and selected bonds and angles are reported in Tables 1 and 2, respectively.

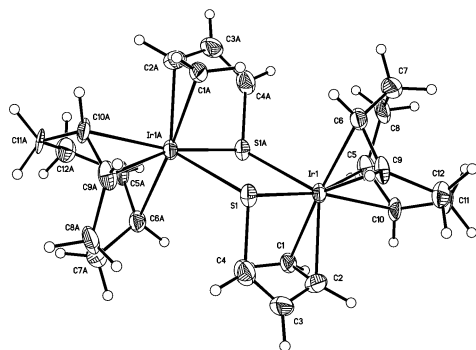


Figure 1. Molecular structure of $[(\eta^4\text{-COD})\text{Ir}(\mu_2\text{-1-2,5-CH}_2\text{CHCHCHS})_2]$ (**5**).

The dimer sits on a crystallographic inversion center located at the midpoint of the C3–C4–C3a–C4a rhombus; thus only half of the molecule is symmetrically independent. Each iridium atom is (1-2,5- η) coordinated to one thiapentadienyl ligand through the C1–C2 and S1 and η^4 -coordinated to one cyclooctadiene ligand. The structure is held together by the two thiapentadienyl ligands, which bridge through the sulfur atoms both iridium centers. According to the bond angles, the geometry of **5** is distorted trigonal-bipyramidal [C1–Ir1–S1, 93.8(2)°; C5–Ir1–S1a, 136.9(2)°]. The angle C1–Ir–C6 [175.3(3)°] shows the axial position of the coordinated double bond of thiapentadienyl and cyclooctadiene ligands. In addition, the terminal double bond C1–C2 [1.426(11) Å] of the thiapentadienyl ligand coordinates to Ir1, while the internal double bond C3–C4 [1.327(14) Å] remains uncoordinated. The bond length of C4–S is 1.762(8) Å. The iridium atom coordinates the nonconjugated double bonds of the COD

Table 1. Crystal Data of Compounds **5** and **9**

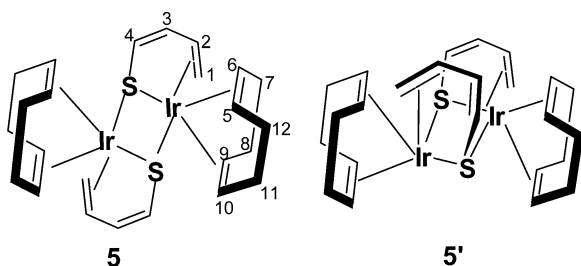
	5	9
molecular formula	$\text{C}_{24}\text{H}_{38}\text{Ir}_2\text{S}_2$	$\text{C}_{24}\text{H}_{34}\text{Ir}_2\text{O}_2\text{S}_2$
mol wt	775.06	401.52
space group	$P\bar{1}$	$P2_1/n$
<i>a</i> (Å)	6.9771(2)	7.9245(3)
<i>b</i> (Å)	7.6804(2)	12.1003(5)
<i>c</i> (Å)	10.9819(3)	12.4320(5)
α (deg)	108.7530(1)	90.00
β (deg)	97.8670(10)	103.6520(1)
γ (deg)	94.9330(10)	90.00
<i>V</i> (Å ³)	546.67(3)	1158.41(8)
<i>Z</i>	1	2
cryst size (mm)	0.17 × 0.15 × 0.08	0.125 × 0.100 × 0.075
<i>D</i> _{calc} (g cm ⁻³)	2.342	2.302
limit θ	7.62–55.04	6.92–54.86
ranges	–9 ≤ <i>h</i> ≤ 8	–10 ≤ <i>h</i> ≤ 10
<i>h, k, l</i>	–9 ≤ <i>k</i> ≤ 9	–15 ≤ <i>k</i> ≤ 14
	–14 ≤ <i>l</i> ≤ 14	–16 ≤ <i>l</i> ≤ 16
total no. of data	7310	4934
total no. of unique data	2470	2625
	(<i>R</i> _{int} = 0.0850)	(<i>R</i> _{int} = 0.0751)
final <i>R</i> 1	0.0418	0.0438
final <i>wR</i> 2	0.1002	0.0865
GOF	1.034	0.971

ligand: C5–C6 [1.453(11) Å] and C9–C10 [1.405(11) Å]. The bond lengths of Ir–S are 2.3788(18) and 2.4900(17) Å. The C1–C2, C3–C4, C4–S, and Ir1–S1 bond lengths of the mononuclear compound $[\text{Ir}(1\text{-}2,5\text{-}\eta\text{-CH}_2\text{CHCHCHS})\text{-}(\text{PMe}_3)_3]$ show for the thiapentadienyl ligand similar data [C1–C2, 1.441(15); C3–C4, 1.316(18); C4–S, 1.758(11); Ir–S, 2.417(2) Å],⁴ where the Ir–S bond length shows an intermediate value compared to the corresponding values of **5**. The more symmetric octahedral complex $[\text{Cp}^*\text{Ir}(\mu_2\text{-SH})\text{SH}]_2$ shows shorter and more symmetric Ir–S bonds [2.380(4) and 2.386(4) Å].²¹

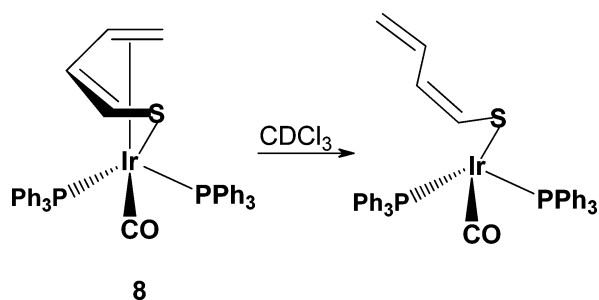
In the solid state compound **5** is in the *anti* configuration, thereby minimizing steric crowding, while in solution the ¹H NMR spectrum of crystals of **5** shows, in CDCl_3 , a mixture of isomers $[(\eta^4\text{-COD})\text{Ir}(\mu_2\text{-1-2,5-CH}_2\text{CHCHCHS})_2]$ (**5** and **5'**) in a 1:5 ratio, Scheme 2.

Table 2. Selected Bond Lengths and Angles of Compounds **5** and **9**

bond length (Å)	5	9	bond angles (deg)	5	9
C(1)–C(2)	1.426(11)	1.440(13)	C(1)–C(2)–C(3)	118.5(7)	115.7(9)
C(2)–C(3)	1.472(13)	1.469(13)	C(2)–C(3)–C(4)	122.6(7)	124.4(9)
C(3)–C(4)	1.327(14)	1.325(14)	C(3)–C(4)–S(1)	119.8(6)	117.5(7)
C(4)–S(1)	1.762(8)	1.777(9)	C(4)–S(1)–Ir(1)	99.8(3)	101.2(3)
C(1)–Ir(1)	2.142(7)	2.168(10)	C(1)–Ir(1)–S(1)	93.8(2)	94.6(3)
C(2)–Ir(1)	2.178(7)	2.178(9)	C(2)–Ir(1)–S(1)	83.1(2)	83.8(3)
Ir(1)–S(1A)	2.4900(17)	2.444(3)	C(5)–Ir(1)–S(1)	87.0(2)	88.3(3)
Ir(1)–S(1)	2.3788(18)	2.329(2)	C(6)–Ir(1)–S(1)	90.6(2)	93.8(3)
C(5)–Ir(1)	2.144(6)	2.151(10)	C(9)–Ir(1)–S(1)	162.8(2)	163.4(3)
C(6)–Ir(1)	2.154(7)	2.109(9)	C(10)–Ir(1)–S(1)	158.4(2)	158.7(3)
C(9)–Ir(1)	2.181(7)	2.210(8)	C(1)–Ir(1)–C(2)	38.5(3)	38.7(4)
C(10)–Ir(1)	2.205(7)	2.230(8)	C(1)–Ir(1)–C(5)	139.1(3)	138.6(4)
C(5)–C(6)	1.453(11)	1.413(14)	C(1)–Ir(1)–C(6)	175.3(3)	171.1(4)
C(6)–C(7)	1.517(11)	1.520(14)	C(1)–Ir(1)–C(9)	95.0(3)	93.0(4)
C(7)–C(8)	1.529(12)	1.521(15)	C(1)–Ir(1)–C(10)	86.7(3)	84.9(4)
C(8)–C(9)	1.524(12)	1.504(15)	C(2)–Ir(1)–C(5)	101.4(3)	101.1(4)
C(9)–C(10)	1.405(11)	1.411(14)	C(2)–Ir(1)–C(6)	140.9(3)	139.8(4)
C(10)–C(11)	1.500(11)	1.510(14)	C(2)–Ir(1)–C(9)	112.7(3)	111.1(4)
C(11)–C(12)	1.505(12)	1.512(14)	C(2)–Ir(1)–C(10)	83.9(3)	82.6(4)
C(12)–C(5)	1.499(11)	1.517(14)	C(1)–Ir(1)–S(1A)	82.8(2)	85.5(3)
S(1)–O(1)		1.505(7)	C(5)–Ir(1)–S(1A)	136.9(2)	135.1(3)
			Ir(1)–S(1)–Ir(1A)	100.99(6)	102.12(8)
			Ir(1)–S(1)–O(1)		116.8(3)

Scheme 2. Mixture of *anti* and *syn* Isomers **5** and **5'**

Scheme 3



The same ^1H NMR spectrum was observed independently of the temperature (room temperature or $50\text{ }^\circ\text{C}$), which may suggest the presence of two dimer isomers **5** and **5'** involving an *anti*–*syn* isomerization associated with the sulfur bridging groups, which has already been documented for thiolato- and hydrosulfide-bridged complexes.²² Full assignment could be done for **5'**, while **5** showed overlapped signals for H1, H2, and most of the COD hydrogens, Table 3. The $^{13}\text{C}\{^1\text{H}\}$ NMR spectroscopy, in Table 4, clearly shows the presence of **5** and **5'**. The iridium-coordinated carbons C1 and C2 resonate at δ 41.00, 41.19 and 63.56, 63.49 for **5** and **5'**, respectively, while the uncoordinated carbons C3 and C4 appear downfield at δ

143.73, 139.57 and 123.01, 121.93; see the Supporting Information. The mass spectrum shows the molecular ion of **5** at 772, along with several fragmentations of the dimer, where the base peak at m/z 384 corresponds to the molecular weight of half of the dimeric complex.

Treatment of **5** with two equivalents of PMe_3 produced $[(\eta^4\text{-COD})\text{Ir}(1\text{-}2,5\text{-}\eta\text{-CH}_2\text{CHCHCHS})\text{PMe}_3]_2$ (**6**) in 53% yield, Scheme 1. The yellow solid melts at $78\text{--}79\text{ }^\circ\text{C}$ and is soluble in hexane. The ^1H and ^{13}C NMR (Tables 3 and 4) supported the preferred U conformation, the same $\eta^{2,1}$ -bonding mode of the thiapentadienyl ligand, and the coordination of the PMe_3 , which in the ^{31}P NMR showed a singlet at -54.5 ppm, quite close to that of free phosphine. The mass spectrum corroborates the molecular ion of the 18-electron derivative **6** at m/z 462.

The synthesis of $\text{Ir}(1\text{-}2,5\text{-CH}_2\text{CHCHCHS})(\text{CO})(\text{PPh}_3)_2$ (**8**) is described in Scheme 1. The cream solid was isolated from reaction of $\text{Ir}(\text{CO})(\text{Cl})(\text{PPh}_3)_2$ (**7**) with potassium thiapentadienide in THF in 82% yield. ^1H and ^{13}C NMR spectra (Tables 3, 4) exhibit the pattern of resonances that is characteristic of the 1-2,5- η -thiapentadienyl bonding mode, which is the preferred coordination mode in the chemistry of thiapentadienyl-iridium^{2,4,11,15,23–27} or rhodium^{28–30} compounds. The ^{31}P NMR (Table 4) shows two doublets from magnetically nonequivalent phosphines at -7.76 (d, $J = 37.2$ Hz) and -1.41 (d, 37.2 Hz). The presence of coordinated CO was confirmed by IR, where a strong peak at 1982 cm^{-1} suggests that the thiapentadienyl ligand reduced the capability of back-bonding of the CO compared to the CO in the Vaska catalyst **7** (1954 cm^{-1}). The mass spectrum, through the FAB technique, affords a molecular ion at $830\text{ }m/z$ for **8**.

Contrastingly, reaction of **7** with potassium pentadienide produces exclusively $\text{Ir}(1\text{-}3\text{-}\eta\text{-pentadienyl})(\text{CO})(\text{PPh}_3)_2$, and the 1-2,5- η -coordination mode is observed only when potassium 2,4-dimethylpentadienide is used. The last one affords an equilibrium mixture of $[\text{Ir}(1\text{-}2,5\text{-}\eta\text{-}2,4\text{-}$

Table 3. $^1\text{H NMR}^a$ of Compounds **5**, **6**, **8**, **10**–**12**, **14Me**, and **14**–**23**

	HI, HI'	H2	H3	H4	H5	H6	H7	H8	H9	H10	H11	H12	Me, Ph, COD
5	1.85 (d, 7.7) ^b 1.67 (d, 8.4)	4.96 ^b	6.33 (dd, 3.9, 5.4)	5.65 (d, 6.2)	3.52 ^b (m)	3.40 (m)	1.97–2.50 ^b (m, 2H)	1.29–1.44 ^b (m) 1.97–2.50 ^b (m)	2.60–2.82 ^b (m)	3.67 ^b (m)	1.97–2.50 ^b (m) 2.60–2.82 ^b (m)	1.60–1.78 ^b (m) 1.97–2.05 ^b (m)	
5'	1.42 (d, 7.7) 1.67 (d, 8.4)	4.96 (dt, 3.7, 8.4)	5.94 (dd, 3.7, 5.9)	5.31 (d, 5.9)	3.52 (m)	3.18 (m)	1.97–2.50 (m, 2H)	1.29–1.44 (m) 1.97–2.50 (m)	2.60–2.82 (m)	3.67 (m)	1.97–2.50 (m) 2.60–2.82 (m)	1.60–1.78 (m) 1.97–2.05 (m)	
6	1.36–1.44 (m)	4.58 (m)	5.74 (m)	5.55 (m)	2.92 (m)	3.75 (m)	2.3–2.8 (m, 2H)	1.40 ^b (m) 2.22 (m)	2.30 (m)	3.37 (m)	2.00–2.50 (m, 2H)	2.05 (m) 2.55 (m)	1.68 (d, 9.2)
8	1.85 (d, 8.1) 2.60 (br)	4.16 (br)	5.72 (br)	5.45 (d, 6.2)									7.24 (m, 15H) 7.31 (m, 15H)
10^c	2.08 (d, 9.2) 2.86 (d, 8.0)	4.61 (m)	6.12 (dd, 4.2, 6.7)	5.83 (d, 6.7)	3.97 (m)	3.74 ^b (m)	2.07 ^b (m) 2.35 ^b (m)	1.85 (m) 2.35 ^b (m)	3.74 ^b (m)	4.86 (m)	2.35 ^b (m)	2.68 (m)	
11^c	2.09 (d, 9.3) 2.85 (d, 8.0)	4.61 (dt, 4.4, 8.4)	6.12 (dd, 4.3, 6.9)	5.83 (d, 6.9)	3.97 (m)	3.75 ^b (m)	2.07 ^b (m) 2.35 ^b (m)	1.85 (m) 2.49 (m)	3.75 ^b (m)	4.86 (dt, 4.2, 8.2)	2.35 ^b (m)	2.68 (m)	
12	2.34 (d, 7.7) 2.56 (d, 9.2)	4.34 (dt, 4.3, 8.3)	6.31 (dd, 3.2, 6.8)	5.99 (d, 7.0)	4.54 (t, 7.0)	3.85 ^d (m)	2.21 (m)	1.93 (m) 2.50 (m)	3.45 ^d (m)	4.88 (t, 8.4)	2.44 (m)	2.78 (m)	1.36 (m, br, 2H, CH ₂) 1.46 (m, br, 2H, CH ₂) 2.21 (m, br, 4H, CH ₂) 3.96 (m, br, 2H, CH) 4.09 (m, br, 2H, CH) 1.81 (m, 4H, 4H, CH ₂) 2.25 (m, 4H, 4H, CH ₂) 4.17 (s, br, 4H, CH)
12^c	2.07 (d, 9.0) 2.84 (d, 8.3)	4.60 (dt, 4.6, 9.2)	6.12 (dd, 3.8, 6.8)	5.83 (d, 6.1)	3.95 (m)	3.76 ^d (m)	2.32 (m) 2.41 (m)	1.86 (m) 2.50 (m)	3.72 ^d (m)	4.85 (m)	2.71 (m, 2H)	2.28 (m) 2.48 (m)	
12^c	2.31 (d, 7.8) 2.46 (d, 9.2)	4.43 ^b (m)	6.34 (m)	5.97 (d, 6.9)	4.43 ^b (m)	3.67 ^d (m)	2.20–2.60 (m)	1.90 (m) 2.20–2.60 (m)	3.54 ^d (m)	4.81 (t, 7.3)	2.74 (m)	2.20–2.60 (m)	
14	1.95 (t, 9.0) 2.02 (dd, 6.6, 7.9)	4.18 (sept, 4.0, 8.6)	6.24 (dt, 3.9, 6.6)	5.76 (d, 6.6)	4.00 ^b (m)	3.73 (m)	2.75 ^b (m, 2H)	1.66 (m) 2.25 (m)	2.73 ^b (m, 2H)	3.98 ^b (m)	2.52 (m) 3.03 (m)	1.68 (m) 2.35 (m)	
14^c	1.64 (t, 8.6, 9.1) 2.12 (t, 6.4, 7.0)	4.13 (m)	6.24 (dt, 4.4, 7.2, 8.0)	5.60 (d, 6.9)	3.39 (m)	3.39 (m)	2.67 (m, 2H)	1.60 (m) 2.25 (m)	2.85 (m)	4.13 (m)	2.54 (m) 2.92 (m)	1.56 (m) 2.25 (m)	1.72 (d, 9.7, 3H)
14Me	1.38 (d, 6.2) 2.85 (m)	3.93 (dd, 8.8)	2.20 (s)	5.58 (s)	3.98 (m)	3.68 ^b (m)	2.77 (m, 2H)	1.74 (m) 2.24 (m)	3.70 ^b (m)	3.79 (m)	2.48 (m) 2.90 (m)	1.84 (m) 2.42 (m)	1.84 (d, 9.7, 3H)
15	2.12 (t, 9.5) 2.20 (t, br)	4.29 (sept, 4.4, 8.4)	6.26 (dt, 4.0, 7.2)	5.86 (d, 6.9)	4.05 (sept, 4.0, 8.8)	3.86 (m)	2.47 (m, 2H)	1.36 (m, 2H)	2.77 (m)	3.37 (m)	2.54 (m, 2H)	1.74 (m) 1.80 (m)	2.07 (d, 9.9, 3H) 2.30 (d, 9.2, 3H) 7.42 (m, 1H) 7.48 (m, 2H) 7.57 (m, 2H)
16	2.33 ^b (m, 2H)	4.44 (m)	6.20 (dt, 4.0, 7.1)	5.79 (d, 6.8)	4.21 (m)	4.05 (m)	2.30 ^b (m) 2.57 (m)	1.58 (m, 2H)	2.91 (m)	3.43 (m)	2.07 (m) 2.39 (m)	2.51 (m, 2H)	2.45 (d, 9.1, 3H) 7.39 (m, 3H)

Table 3. continued

	H1, H1'	H2	H3	H4	H5	H6	H7	H8	H9	H10	H11	H12	Me, Ph, COD
17	2.35 (t, 9.0) 2.81 (t, 6.3)	4.65 (sept, 4.2, 8.6)	6.15 (dt, 4.5, 7.2)	5.74 (d, 6.9)	4.07 (m, br)	4.20 ^b (m, br)	2.30 (m, br) 2.60 (m, br)	1.27 (m) 1.62 (m, br)	3.21 (m, br)	4.20 ^b (m, br)	1.87 (m) 2.53 ^b (m, br)	2.03 (m, br) 2.53 ^b (m, br)	7.49 (m, 5H) 7.96 (t, 8.0, 8.9, 2H)
18	2.17 (d, 9.2) 2.62 (d, 8.4)	4.43 (dt, 4.0, 8.8, 9.2)	5.94 (dt, 4.4, 7.0)	5.73 (d, 6.9)	4.17 (m)	3.87 (t, 6.9)	1.99 (m) 2.30 (m)	1.76 (m, 2H)	3.50 ^b (m)	4.88 (dt, 8.0, 8.8)	2.25 (m, 2H)	2.62 ^b (m) 2.75 (m)	7.41 (s, br, 9H) 7.70 (m, 6H)
19	2.51 (dd, 1.7, 7.9)	4.31 (dt, 4.1, 8.2, 9.0)	6.35 (dd, 4.1, 6.8)	5.70 (d, 6.8)	4.63 (dt, 4.7, 8.6)	4.20 (t, 7.2)	2.95 (m) 3.27 (dd, 7.7)	1.74 (m) 2.33 (m)	3.19 (q, 8.0)	4.80 (t, 7.4)	2.73 (m) 2.99 (m)	2.05 (m) 2.65 (m)	3.34 (s, br, 3H) 3.46 ^d (s, br, 3H)
19 ^f	2.72 (d, 8.1) 2.90 ^b (m)	4.55 (dt, 4.1, 8.1, 9.3)	6.40 (dd, 4.0, 7.0)	5.55 (d, 7.0)	4.45 (m)	4.00 (t, 7.0)	3.30 (d, 7.8) 3.35 (d, 8.1)	1.81 (m) 2.39 (m)	3.49 (q, 8.0)	5.07 (t, 7.4)	2.85 (m) 3.05 (m)	2.15 (m) 2.70 ^b (m)	
20	5.02 (d, 9.3) 5.06 (dd, 2.0, 17.0)	7.22 (dt, 7.1, 17.0)	6.02 (dt, 10.3, 12.0)	5.99 (dt, 10.5, 12.0)	3.20 (s, br)	3.20 (s, br)	2.23 ^d (m)	2.40 ^d (m)	3.20 (s, br)	3.20 (s, br)	2.40 ^d (m)	2.23 ^d (m)	1.62 (m, 18H)
21					3.14 (s, br)	3.14 (s, br)	1.72 (m) 2.24 (m)	1.84 (m) 2.19 (m)	4.95 (m)	4.95 (m)	1.84 (m) 2.19 (m)	1.72 (m) 2.24 (m)	1.41 (d, 9.5, 9H)
21 ^g					2.87 (m)	2.87 (m)	1.19 (m) 2.02 (m)	1.53 (m) 2.02 (m)	5.33 (m)	5.33 (m)	1.53 (m) 2.02 (m)	1.19 (m) 2.02 (m)	0.93 (d, 9.5, 9H)
22					2.73 (s, br)	2.73 (s, br)	1.60 (m) 2.22 (m)	1.88 (m) 2.22 (m)	5.19 (s, br)	5.19 (s, br)	1.88 (m) 2.22 (m)	1.60 (m) 2.22 (m)	7.42 (s, br, m, p) 7.70 (m, o, m)
23					3.21 (s, br)	3.21 (s, br)	2.23 ^d (m)	2.23 ^d (m)	3.21 (s, br)	3.21 (s, br)	2.38 ^d (m)	2.38 ^d (m)	1.63 (m, 18H)

^aIn CDCl₃, δ in ppm and *J* in hertz. For numbering see Schemes 1, 2, and 4 and Figures 1, 3–9. ^bOverlapped signals. ^cDMSO-*d*₆. ^dAssignment may be reversed. ^eTDF. ^fAcetone-*d*₆. ^gC₆D₆.

Table 4. $^{13}\text{C}\{\text{H}\}$, ^3P , and ^7Li NMR^a of Compounds 5, 6, 8, 10–12, 14Me, and 14–23

	C1	C2	C3	C4	C5	C6	C7	C8	C9	C10	C11	C12	Me, Ph, CO	^3P , ^7Li
5	41.00	63.56	143.73	123.01	62.09	66.79	39.48	28.44	81.93	81.42	35.80	29.47		
5	41.19	63.49	139.57	121.93	60.93	66.55	39.23	27.52	79.58	78.61	35.07	29.74		
6	30.90	60.58	129.60	129.10	62.23	66.00	35.63	31.39	83.96	70.81	34.79	33.38	17.10 (d, 31.1)	−54.5
8	31.70 (br)	58.58 (br)	130.79 (br)	129.10 (br)									174.28 (t, 6.1, 6.9, CO) 127.75 (d, 32.2, m) 129.48 (s, p) 133.89 (d, 59.2, o) 136.03 (d, 43.8, i)	−1.41 (d, 37.2) −7.76 (d, 37.2)
10^b	41.13	62.05	138.90	140.70	67.60	68.50	33.20	29.90	109.70	101.00	31.40	31.00		4.2
11^{b,c}	41.68 (t, 157.6)	62.60 (dd, 123.0)	168.4, 139.51 (d, 161.4)	141.20 (d, 177.6)	68.19 (d, 161.4)	68.61 (d, 157.5)	33.74 (t, 127.6)	30.38 (t, 126.1)	110.25 (d, 159.9)	101.57 (d, 162.2)	32.01 (t, 127.6)	31.62 (t, 123.7)		
12	46.85	59.59	135.66	144.05	71.07	70.03	37.83	27.15	102.85	96.14	33.86	28.51	62.78, 63.35 (CH) 57.00, 57.36 (CH) 31.91, 32.11 (CH ₂) 30.65, 30.88 (CH ₂) 74.27 (br, CH) 31.33 (br, CH ₂)	
12^b	41.67	62.60	139.52	141.21	68.18	69.11	33.75	30.40	110.25	101.56	32.03	31.61		
14	36.03 (d, 6.7)	57.77 (d, 14.5)	139.08 (d, 2.1)	142.94 (d, 4.1)	66.38 (d, 11.4)	68.16 (d, 6.2)	36.41 (d, 4.7)	29.38	100.37 (d, 2.6)	82.47 (d, 2.0)	34.50 (d, 6.2)	30.38	16.89 (d, 31.1)	−51.7
14Me	49.70 (d, 6.2)	66.33 (d, 13.8)	151.90	136.24	68.06 (d, 12.3)	66.73 (d, 6.2)	36.07 (d, 4.6)	29.38	96.41	81.21	33.76 (d, 6.2)	30.82	17.85 (d, 4.6, Me1) 19.07 (d, 4.6, Me3) 16.61 (d, 30.8, PMe ₃)	−49.8
15	37.05 (d, 6.9)	58.87 (d, 14.6)	138.77	143.27 (d, 4.5)	67.75 (d, 11.6)	68.04 (d, 6.2)	35.34	28.78	100.93	89.00	33.58 (d, 4.7)	31.44	12.92 (d, 30.0) 15.57 (d, 33.1) 128.73 (d, 8.4, m) 129.72 (s, p) 129.74 (d, 7.7, o)	−39.0
16	39.90 (d, 7.2)	61.07 (d, 14.0)	137.73	143.15 (d, 3.5)	68.79 (d, 12.0)	68.12 (d, 5.5)	33.90	30.73	101.87	92.76	32.17	31.84 (d, 3.4)	16.10 (d, 32.4) 133.24 (d, 10.0, o) 131.19 (d, 7.8, o) 130.14 (s, p) 129.33 (s, p) 128.33 (t, 10.0, m)	−28.0
17	43.49 (d, 7.9)	63.39 (d, 13.6)	137.16 (d, ~1.0)	142.96 (d, 4.3)	67.92 (d, 12.9)	71.52 (d, ~3)	33.32	29.89	100.21	93.91	32.73	32.43	128.10 (d, 9.5, m) 129.74 (d, 2.2, p) 134.55 (d, 9.4, p)	−8.1

Table 4. continued

	C1	C2	C3	C4	C5	C6	C7	C8	C9	C10	C11	C12	Me, Ph, CO	³¹ P, ⁷ Li
18	40.85	62.32	139.13	140.57	69.70	70.53	33.35	30.35	110.00	102.26	32.19	31.68	135.15 (d, 17.4, i)	
19	40.71	58.97	138.42	141.68	75.69	76.49	37.67	27.27	103.59	93.41	36.94	27.74	45.49 47.10 176.76	
19 ^d	41.17	59.78	138.01	142.05	75.08	75.91	37.95	26.70	104.86	95.16	37.08	27.57	178.83	
20	116.88	134.30	127.56	153.45	68.60 (d, s, 3)	68.60 (d, s, 3)	34.18 (br)	34.18 (br)	68.60 (d, s, 3)	68.60 (d, s, 3)	34.18 (br)	34.18 (br)	20.02 (m)	-52.4
21					51.37	51.37	29.20	33.95 (d, 3.8)	93.38 (d, 14.6)	93.38 (d, 14.6)	33.95 (d, 3.8)	29.20	12.82 (d, 34.6)	-16.1
22					54.03	54.03	29.97 (d, 2.1)	33.90 (d, 3.2)	94.44 (d, 14.3)	94.44 (d, 14.3)	33.90 (d, 3.2)	29.97 (d, 2.1)	128.53 (d, 10.2, m)	23.2
23					68.57 (m, 3.9, 5.4)	68.57 (m, 3.9, 5.4)	34.21	34.21	68.57 (m, 3.9, 5.4)	68.57 (m, 3.9, 5.4)	34.21	34.21	130.79 (d, 2.3, p)	-52.4
													130.96 (s)	
													131.63 (s)	
													135.43 (d, 11.0, o)	
													20.16 (m, 3.1, 3.8, 4.6)	

^aIn CDCl₃, δ in ppm and J in hertz. For numbering see Schemes 1, 2, and 4 and Figures 1, 3–9. ^bDMSO-*d*₆. ^cCoupled. ^d(CD₃)₂CO.

dimethylpentadienyl)(CO)(PPh₃)₂] and [Ir(1-3-η-2,4-dimethylpentadienyl)(CO)(PPh₃)₂] in which, in methylene chloride at 20 °C, the 1-3-η-pentadienyl complex predominates slightly (1.5:1.0).³¹

A preliminary ¹H and ³¹P NMR study of **8** in CDCl₃, at room temperature and after 22 days, showed the transformation of the thiapentadienyl ligand from 1- to 2,5-η- into 5-η-.³² In the latter, an S conformation was observed in solution and a singlet at ³¹P δ 2.33; see Scheme 3 and Supporting Information.

B. Sulfinylpentadienyl Chemistry. The corresponding sulfinylpentadienyl complex [(η⁴-COD)Ir(μ₂-1-2,5-η-CH₂CHCHCHSO)]₂ (**9**) can be prepared using a similar procedure to that described for the thiapentadienyl analogue **5** (Scheme 1). However, manipulating the sulfinylpentadienyl salt **2M** (M = Li, Na, K) is much more complicated, because it easily suffers a dismutation to butadienesulfinate and thiapentadienide, depending on the stability of the sulfinylpentadienyl, which decreases in the following order: **2K** > **2Na** > **2Li**.¹⁹ Considering the longer time observed for the dismutation of **2K**, the synthesis of **9** was carried out, forming *in situ* **2K** from 2,5-dihydrothiophene-1-oxide and KH in the presence of **4**. After 30 min, the mixture was filtered, evaporated, and recrystallized from methylene chloride/diethyl ether, which gave yellow crystals of **9** in very low yield (≈5 mg). The ¹H NMR of the sulfinylpentadienyl ligand confirms the coordination of H1 and H2 (2.17 and 3.12 ppm) and noncoordination of H3 and H4 (5.99 and 6.84 ppm); the COD signals are overlapped and were not assigned. The crystal structure of **9** (Tables 1 and 2, Figure 2) was established, showing a dimeric structure, analogous to **5**.

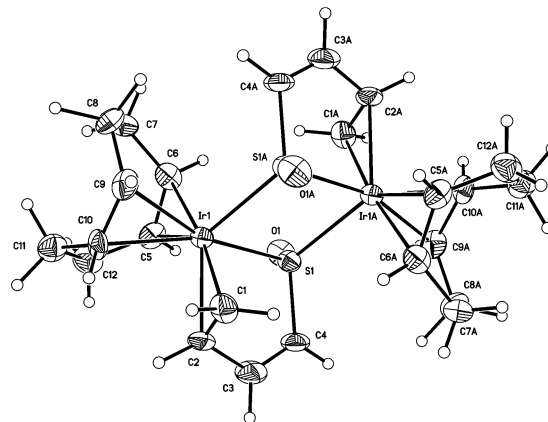


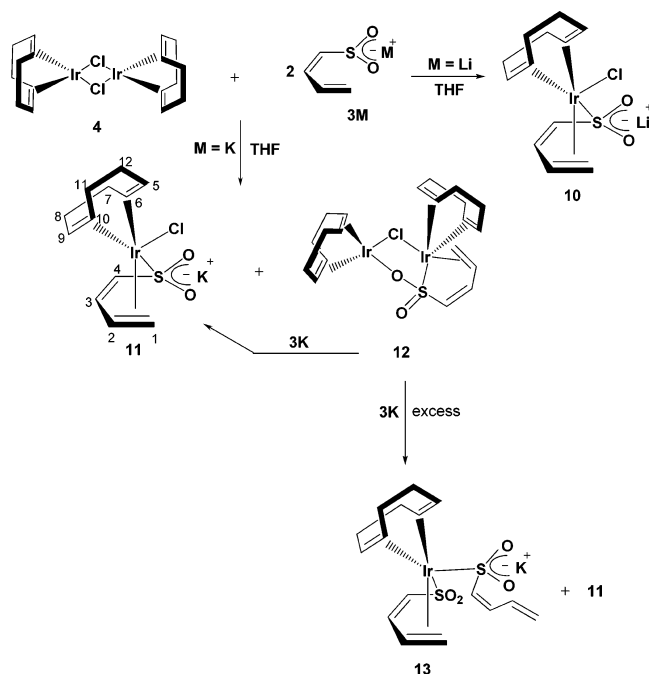
Figure 2. Molecular structure of [(η⁴-COD)Ir(μ₂-1-2,5-CH₂CHCHCHSO)]₂ (**9**).

The Ir–S bond lengths [2.329(2) and 2.444(3) Å] are shorter than those of **5** [2.3788(18) and 2.4900(17) Å], where the corresponding longer bond lengths of **9** and **5** are attributed to the coordination bond from the nonbonding lone pair of the sulfur that interacts with the iridium atom to give a dimer. Comparison between **9** and DMSO complexes, M = Ru(II), Os(II), Pd(II), Pt(II), Pt(IV) [2.217(2)–2.343(3) Å],³³ shows that Ir(I) is in the highest value range. The bond length S=O is 1.505(7) Å, which is similar to the average value of noncoordinated sulfoxides and among the highest top values of reported bond lengths of S=O bonds in DMSO complexes, where coordination is through the sulfur atom (1.42–1.512 Å).³³ The bond angle in **9** suggests a distorted trigonal-bipyramidal geometry, where C1–C2 and C5–C6 are in axial

positions [C1–Ir1–C6, 171.1(4)°] and the sulfur atom [C1–Ir1–S1, 94.6(3)°] is almost perpendicular to C1–C2. Due to the presence of the oxygen atom on the sulfur, the bond angles of the sulfynylpentadienyl ligand in **9** [C1–C2–C3, 115.7(9)°; C2–C3–C4, 124.4(9)°; C3–C4–S1, 117.5(7)°] show the greatest deviation compared to the thiapentadienyl analogue **5** [C1–C2–C3, 118.5(7)°; C2–C3–C4, 122.6(7)°; C3–C4–S1, 119.8(6)°] and the typical free diene (120°).

C. Butadienesulfonyl Chemistry. $[(\eta^4\text{-COD})\text{IrCl}(1\text{-}2,5\text{-}\eta\text{-CH}_2\text{CHCHCHSO}_2\text{M}^+)]$. The synthesis of compounds $[(\eta^4\text{-COD})\text{IrCl}(1\text{-}2,5\text{-}\eta\text{-CH}_2\text{CHCHCHSO}_2\text{M}^+)]$ (M = Li, **10**; M = K, **11**) was carried out by mixing compound **4** and two equivalents of the salts **3M** (M = Li, K) suspended in THF at room temperature, Scheme 4.

Scheme 4



In each case, the product or reaction showed a transparent amber solution, from which product **10** or **11** could be isolated in 69% and 66% yield, respectively. The formation of a dimeric structure, such as $[(\eta^4\text{-COD})\text{Ir}(\text{Cl})(5\text{-}\eta\text{-CH}_2\text{CHCHCHSO}_2\text{Li})_2]$, analogous to the Cp*Ir derivatives¹⁵ described in the Introduction, or the mononuclear ion-pair complex $[(\eta^4\text{-COD})\text{IrCl}(1\text{-}2,5\text{-}\eta\text{-CH}_2\text{CHCHCHSO}_2\text{Li}^+)]$ (**10**) such as those found in Cp*Ru³⁴ and Cp*Rh³⁵ chemistry could be expected. On the basis of the mass spectra and without crystallographic evidence, we describe the structure as mononuclear ion-pair **10**.

The mass spectrum of **10** shows a molecular ion at 460 m/z assigned to $[\text{10}]^+$, along with fragments at 425, 418, 352, and 316 m/z as a consequence of losing Cl, LiCl, and COD (Cl and COD), respectively. This detailed pattern differs from that found in previous dinuclear compounds prepared with the Cp*Ir fragments (M = Rh, Ir), which are quite fragile in the mass spectrometry experimental conditions. However, preliminary experiments via dynamic laser-light scattering of **10**, **11**, and $(\eta^4\text{-COD})\text{Ir}(1\text{-}2,5\text{-}\eta\text{-CH}_2\text{CHCHCHSO}_2)\text{PPh}_3$ (**17**) (*vide infra*) showed a monodisperse mixture for **17** (250–550 nm) and polydisperse mixtures for **10** (0.5–10.0 and 70–6000 nm)

and **11** (0.5–75.0 and 80–6000 nm). The tendency to favor polydisperse aggregates was higher in the lithium derivative (predominates between 70 and 6000 nm) compared to that shown by the potassium (predominates at 0.5–75.0 nm), which suggests that some kinds of oligomers, with the same empirical formula, cannot be discriminated in the case of **10** and **11**; see the Supporting Information.

The IR spectra showed strong bands for O=S=O vibrations of **10** (ν_{as} 1133, 1108 and ν_{s} 1029 cm^{-1}) and **11** (ν_{as} 1146, 1108 and ν_{s} 1041 cm^{-1}); those for **10** were at lower wavenumber than those of **11**. Both ion-pair complexes **10** and **11** were at lower frequencies compared to those of non-ion-pair derivatives, such as $[(\eta^4\text{-COD})\text{Ir}(1\text{-}2,5\text{-}\eta\text{-CH}_2\text{CHCHCHSO}_2)\text{-L}]$ (L = DMSO, **18**: 1166, 1100, 1051 cm^{-1} ; L = CO, **19**: 1171, 1052 cm^{-1} , *vide infra*). This can be attributed to the alkaline metal interaction with the O=S=O fragment in **10** and **11**, *vide infra*. The analogy between NMR spectroscopic data for **3M** (M = Li, Na, K) has been proposed as indicative that the metal is interacting exclusively with the sulfonyl group, in which the charge is delocalized along with the oxygen–sulfur–oxygen atoms.¹⁹ The same trend is also observed here for compounds **10** and **11**. The (1-2,5- η -) bonding mode of the butadienesulfonyl ligand in **10** and **11** was evident from ¹H and ¹³C{¹H} NMR spectroscopy, as described in Tables 3 and 4. In the ¹H NMR spectra, H4 and H3 resonate at a typical olefinic value of δ 5.83 and 6.12, while H1, H1', and H2 are shifted substantially upfield to δ 2.08–2.09, 2.85–2.86, and 4.61, respectively. Similarly, in the ¹³C{¹H} NMR the metal-coordinated carbons C1 and C2 resonate at around δ 41 and 62, respectively, while the uncoordinated carbons C3 and C4 appear downfield at around δ 139 and 141, respectively. The ⁷Li NMR in DMSO-*d*₆ shows a singlet at 4.2 ppm for **10**.

The microanalysis showed one lithium and chloro, or the corresponding potassium and chloro, per each molecule of $(\eta^4\text{-COD})\text{Ir}(1\text{-}2,5\text{-}\eta\text{-CH}_2\text{CHCHCHSO}_2)$ in **10** and **11**, respectively. The isolated product **11**, upon dissolution in CDCl₃, showed a precipitate identified as KCl. The evidence of KCl was unequivocally established in solution by electrochemical detection of Cl[−], as well as the isolation and powder diffraction of the solid, which was filtered from the synthetic reaction of compound **16** (*vide infra*).

Cyclic voltammetry confirmed the formation of the ion-pair $[(\eta^4\text{-COD})\text{IrCl}(1\text{-}2,5\text{-}\eta\text{-CH}_2\text{CHCHCHSO}_2\text{K}^+)]$ (**11**), and an electrochemical experiment was also carried out in order to demonstrate the presence of the potassium cation in **11**; it was possible to trap the cation with 18-crown-6 ether, which shows that there is a proportional response between the current intensity and the concentration of the crown-ether. This suggests that the K⁺ cation was trapped by the ether and released higher concentrations of free **11**[−]; see the Supporting Information.

The higher stability of **3K**, as well as the easier removal of KCl compared to LiCl from **11** and **10** in the presence of donor molecules, determined the use of **11** in the development of the iridium-cyclooctadiene chemistry.

As already mentioned, the reaction of **4** in THF with **3K**, after stirring for 1 h at room temperature, gave a cream powder of **11** in 66% yield. If shorter reaction times (10 min) are used at low temperature (−110 °C) and after evaporating of THF, an intermediate mustard-yellow solid, $(\eta^4\text{-COD})\text{Ir}(\mu\text{-Cl})(1\text{-}2\text{-}\eta\text{-S,O-}\mu\text{-OSOCHCHCHCH}_2)_2\text{Ir}(\eta^4\text{-COD})$ (**12**), is isolated in 60% yield, Scheme 4. Compound **12** showed the butadienesulfonyl ligand bonding in an intermolecular fashion, as a

Table 5. Crystal Data for Iridium Compounds 12, 14, 15, and 17–20

	12	14	15	17	18	19	20
formula	C ₂₀ H ₂₉ ClIr ₂ O ₂ S	C ₁₅ H ₂₆ IrO ₂ PS	C ₂₀ H ₂₈ IrO ₂ PS	C ₃₀ H ₃₂ IrO ₂ PS·CHCl ₃	C ₁₄ H ₂₃ IrO ₃ S ₂ ·2CH ₂ Cl ₂	C ₁₃ H ₁₇ IrO ₃ S	C ₁₈ H ₃₅ IrO ₂ P ₂ S
mol wt	753.34	493.59	555.65	799.15	665.50	445.53	569.66
space group	P2 ₁ /n	P2 ₁ /n	P2 ₁ 2 ₁ 2 ₁	P2 ₁ 2 ₁ 2 ₁	P $\bar{1}$	P2 ₁ /n	P2 ₁ /c
a (Å)	6.89680(10)	11.4365(6)	8.9049(2)	10.1020(2)	9.3620(3)	8.26540(10)	9.5092(2)
b (Å)	15.7763(3)	12.6545(6)	14.1185(3)	14.2439(3)	10.5183(4)	24.3232(4)	14.5052(3)
c (Å)	19.2556(4)	12.5745(7)	15.1554(3)	20.7100(4)	13.1777(6)	13.0908(3)	16.0327(3)
α (deg)	90.00	90.00	90.00	90.00	96.051(2)	90.00	90.00
β (deg)	100.3440(1)	111.603(3)	90.00	90.00	108.552(2)	100.5710(1)	99.7080(10)
γ (deg)	90.00	90.00	90.00	90.00	108.589(2)	90.00	90.00
V (Å ³)	2061.07(7)	1691.99(15)	1905.40(7)	2980.00(10)	1134.71(8)	2587.12(8)	2179.77(8)
Z	4	4	4	4	2	8	4
cryst size (mm)	0.25 × 0.10 × 0.08	0.15 × 0.10 × 0.10	0.35 × 0.15 × 0.15	0.15 × 0.15 × 0.15	0.38 × 0.25 × 0.13	0.40 × 0.30 × 0.20	0.45 × 0.25 × 0.20
D _{calc} (g cm ⁻³)	2.428	1.938	1.937	1.781	1.948	2.288	1.736
limit θ	7.20–54.94	4.74–54.98	7.06–54.94	6.94–54.96	6.62–55.06	5.94–54.96	5.88–54.98
ranges	–8 ≤ h ≤ 8	–14 ≤ h ≤ 14	–11 ≤ h ≤ 11	–12 ≤ h ≤ 13	–12 ≤ h ≤ 11	–10 ≤ h ≤ 10	–11 ≤ h ≤ 12
h, k, l	–20 ≤ k ≤ 18	–15 ≤ k ≤ 16	–18 ≤ k ≤ 15	–18 ≤ k ≤ 15	–13 ≤ k ≤ 13	–31 ≤ k ≤ 29	–18 ≤ k ≤ 18
	–22 ≤ l ≤ 24	–16 ≤ l ≤ 15	–19 ≤ l ≤ 19	–23 ≤ l ≤ 26	–17 ≤ l ≤ 16	–16 ≤ l ≤ 16	–19 ≤ l ≤ 20
total no. of data	18 078	16 094	12 459	18 417	10 319	23 128	26 713
total no. of unique data	4525	3815	4240	6708	5128	5833	4992
	R _{int} = 0.0483	R _{int} = 0.0845	R _{int} = 0.0302	R _{int} = 0.0699	R _{int} = 0.0573	R _{int} = 0.0732	R _{int} = 0.0819
final R1	0.0460	0.0431	0.0197	0.0390	0.0480	0.0372	0.0370
final wR2	0.0569	0.0879	0.0409	0.0691	0.1122	0.0740	0.0839
GOF	1.137	1.054	0.972	1.027	1.030	1.025	1.060

sulfonato-O,S complex,³⁶ which was fully characterized, including the crystal structure, Table 5 and Figure 3.

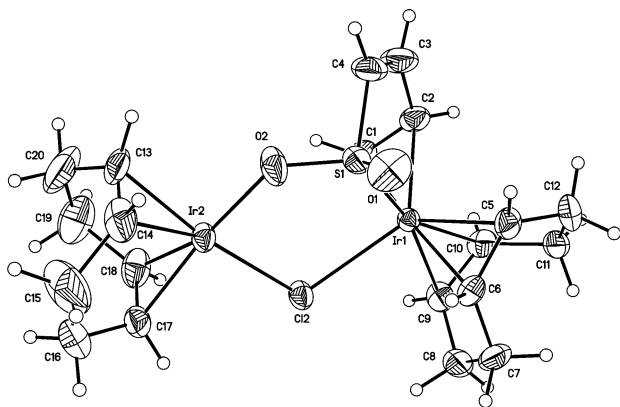


Figure 3. Molecular structure of $[(\eta^4\text{-COD})\text{Ir}(\mu\text{-Cl})(1\text{-}2\text{-}\eta\text{-S,O-}\mu\text{-OSOCHCHCHCH}_2\text{)-Ir}(\eta^4\text{-COD})]$ (**12**).

Compound **12** is formed by a half-molecule of the dimer **4**, which bridges, through the chloro atom, to a $(\eta^4\text{-COD})\text{Ir}(1\text{-}2,5\text{-}\eta\text{-CH}_2\text{CHCHCHSO}_2)$; one oxygen of the butadienesulfonyl ligand also bridges the corresponding $(\eta^4\text{-COD})\text{IrCl}$ fragment. The bond length of S1–Ir1 is particularly short [2.2738(14) Å] compared to that in **14**, **15**, **17**–**20** [average 2.31 Å, Table 6] and Cp*IrCl(1-2,5- $\eta\text{-CH}_2\text{CHCHCHSO}_2$) [2.3091(18) Å]¹² and is even shorter than that in the dimeric structures $[\text{Cp}^*\text{Ir}(\text{Cl})_2\{(5\text{-}\eta\text{-CHRCHCRCHSO}_2)\}(\text{Li})\text{(THF)}_2]$ [average 2.2948 Å]. As expected, S1–O2 [1.507(5) Å] is significantly longer, due to the O2 to Ir2 bridging bond. The bond lengths Ir1–Cl2 [2.5392(14) Å] and Ir2–Cl2 [2.3662(14) Å] are longer and shorter, respectively, than those in **4**, where a range of 2.397–2.407 Å is observed.³⁷

It is also interesting to mention that, in solution, dinuclear compound **12** dissociates in the presence of coordinating solvents, such as DMSO-*d*₆ or THF-*d*₈, while the dinuclear asymmetric structure remains in CDCl₃; see the Supporting Information. IR of **12** shows the corresponding SO₂ vibration bands at 1151 (vs, br), 1107 (s, sh), 1034 (vs), and 1004 (s, sh).

When a suspension of **3K** in THF is added to **12**, there is evidence of formation of **11** along with traces of another complex, tentatively assigned as $(\eta^4\text{-COD})\text{Ir}(1\text{-}2,5\text{-}\eta\text{-CH}_2\text{CHCHCHSO}_2)(5\text{-}\eta\text{-S}(\text{O}_2^-\text{K}^+)\text{CHCHCHCH}_2)$ (**13**), according to the ¹H NMR, which gives evidence of two butadienesulfonyl ligands coordinated to the Ir(COD) fragment in different (1-2,5- $\eta\text{-}$) and (5- $\eta\text{-}$) bonding modes. This reaction was nonselective, showing a mixture of **13**, **3K**, and **11**, from which we could remove **3K**, but were unable to isolate **13** as a pure compound.

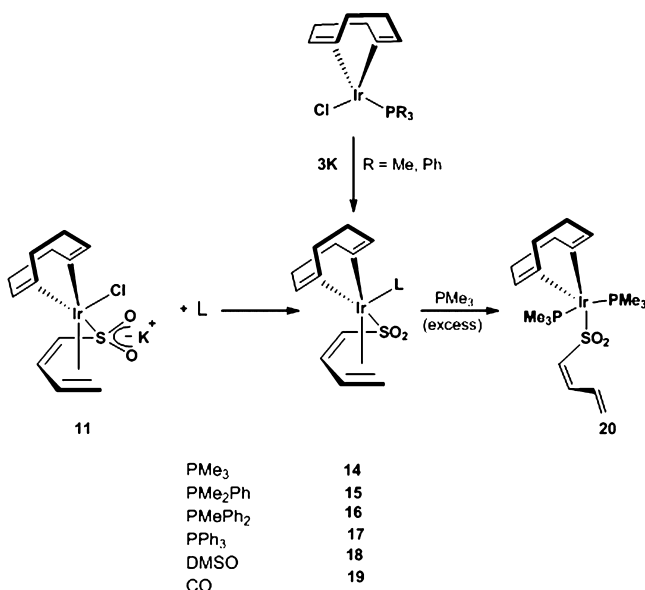
$[(\eta^4\text{-COD})\text{IrCl}(1\text{-}2,5\text{-}\eta\text{-CH}_2\text{CHCHCHSO}_2)\text{L}]$. The series of pentacoordinated Ir(I) complexes of general formula $[(\eta^4\text{-COD})\text{Ir}(1\text{-}2,5\text{-}\eta\text{-CH}_2\text{CHCHCHSO}_2)\text{L}]$ (L = PMe₃, **14**; PMe₂Ph, **15**; PMePh₂, **16**; PPh₃, **17**; DMSO, **18**; and CO, **19**) were prepared, under mild conditions, from **11** and the corresponding ligand L, which shows different σ or π donor–acceptor properties. Compounds **15**–**17**, which are derivatives with aromatic groups in the phosphine ligands, gave the highest yields (44–97%); the lowest yield, **14**, was obtained for the most basic PMe₃ (32%). The σ -donor DMSO affords complex **18** in 55% yield, while the best π -acceptor ligand, CO in complex **19**, required double chromatography, and it was obtained in 60% yield. Compounds **14**–**19** are readily soluble in THF and CHCl₃, Scheme 5.

The disubstituted trimethylphosphine complex $[(\eta^4\text{-COD})\text{Ir}(5\text{-}\eta\text{-SO}_2\text{CHCHCHCH}_2)(\text{PMe}_3)_2]$ (**20**) was obtained by addition of six equivalents of phosphine to compound **14**, Scheme 5. All derivatives **14**–**19** are fairly stable kinetically in

Table 6. Selected Bond Length (Å) for Compounds 12, 14, 15, and 17–20

	12	14	15	17	18	19	20
C(1)–C(2)	1.427(10)	1.426(12)	1.434(6)	1.429(10)	1.415(13)	1.418(9)	1.335(11)
C(2)–C(3)	1.486(9)	1.487(11)	1.484(7)	1.479(10)	1.462(12)	1.487(9)	1.437(11)
C(3)–C(4)	1.314(10)	1.296(12)	1.293(9)	1.294(11)	1.340(12)	1.323(9)	1.330(9)
C(4)–S(1)	1.756(6)	1.747(9)	1.763(6)	1.788(7)	1.758(8)	1.759(7)	1.790(7)
C(1)–Ir(1)	2.153(6)	2.140(7)	2.151(4)	2.177(7)	2.139(8)	2.149(7)	2.3334(13) P(2)–Ir(1)
C(2)–Ir(1)	2.154(6)	2.171(7)	2.191(4)	2.179(7)	2.163(8)	2.176(6)	2.1815(6) P(2)–C(16)
S(1)–O(1)	1.450(5)	1.465(6)	1.459(4)	1.465(4)	1.466(6)	1.457(5)	1.479(5)
S(1)–O(2)	1.507(5)	1.458(6)	1.474(3)	1.468(4)	1.463(7)	1.458(5)	1.466(4)
S(1)–Ir(1)	2.2738(14)	2.3076(19)	2.3123(11)	2.3011(16)	2.3168(18)	2.3106(15)	2.3146(13)
C(5)–Ir(1)	2.136(6)	2.169(8)	2.172(4)	2.175(6)	2.184(8)	2.203(6)	2.190(6)
C(6)–Ir(1)	2.156(6)	2.172(7)	2.174(4)	2.183(5)	2.170(7)	2.198(7)	2.168(5)
C(9)–Ir(1)	2.243(6)	2.292(7)	2.280(4)	2.329(7)	2.301(7)	2.326(6)	2.200(6)
C(10)–Ir(1)	2.254(6)	2.249(8)	2.251(4)	2.280(7)	2.269(8)	2.287(6)	2.229(5)
C(5)–C(6)	1.425(9)	1.426(12)	1.421(6)	1.434(10)	1.401(12)	1.410(9)	1.437(9)
C(6)–C(7)	1.515(9)	1.521(11)	1.516(6)	1.518(9)	1.518(11)	1.520(9)	1.517(9)
C(7)–C(8)	1.528(11)	1.524(12)	1.536(7)	1.518(10)	1.508(14)	1.431(11)	1.521(10)
C(8)–C(9)	1.499(9)	1.518(12)	1.517(7)	1.530(11)	1.519(13)	1.494(10)	1.522(9)
C(9)–C(10)	1.374(9)	1.390(12)	1.385(6)	1.375(10)	1.376(12)	1.372(10)	1.412(9)
C(10)–C(11)	1.520(9)	1.527(14)	1.496(6)	1.504(10)	1.513(14)	1.491(10)	1.498(8)
C(11)–C(12)	1.511(10)	1.529(13)	1.528(6)	1.533(11)	1.510(16)	1.439(11)	1.507(10)
C(12)–C(5)	1.513(9)	1.522(12)	1.525(6)	1.523(10)	1.486(13)	1.526(10)	1.521(9)
P(1)–Ir(1)	2.5392(14) Ir(1)–Cl(2)	2.398(2)	2.3896(10)	2.4563(16)	1.470(6) S(2)–O(3)	1.950(7) C(13)–Ir(1)	2.3731(14)
P(1)–C(13)	2.3662(14) Ir(2)–Cl(2)	1.822(8)	1.815(4)	1.859(6)	1.778(8) S(2)–C(13)	1.119(8) C(13)–O(3)	1.825(6)
P(1)–C(14)	2.078(5) Ir(2)–O(2)	1.816(8)	1.838(5)	1.836(6) P(1)–C(19)	2.4401(18) Ir(1)–S(2)		1.826(6)
P(1)–C(15)	2.101(6) Ir(2)–C(13)	1.821(8)	1.822(4)	1.830(6) P(1)–C(25)	1.774(8) S(2)–C(14)		1.821(6)

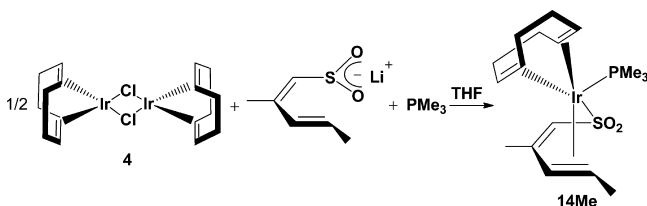
Scheme 5



the solid state, slightly air-sensitive in solution, and thermally stable, while **20** easily dissociates PMe_3 , affording an equilibria with **14** and **20'** (*vide infra*). The phosphine derivatives **14**–**17** and **20** melt sharply, without decomposition, while **18** and **19** melt with decomposition.

Compounds **14**, **15**, **18**, and **19** were prepared *in situ*, using stoichiometric amounts of dimer **4** with 3Na , 3Li , or 3K in the presence of two equivalents of the PMe_3 or PMe_2Ph and excess DMSO or CO. However, better yields can be obtained from the former reaction in which **11** was previously isolated. Also, lower yields were obtained when **10** was used, and because of that, all reactions described here, as already mentioned, will be related to the addition reactions exclusively to compound **11**, except for $[(\eta^4\text{-COD})\text{Ir}(1\text{-}2,5\text{-}\eta\text{-SO}_2\text{CHC}(\text{Me})\text{CHCH}(\text{Me}))\text{-PMe}_3]$ (**14Me**), which was obtained only from reaction of **4** and two equivalents of $\text{Li}[\text{SO}_2\text{CHC}(\text{Me})\text{CHCHMe}]$ and PMe_3 , Scheme 6.

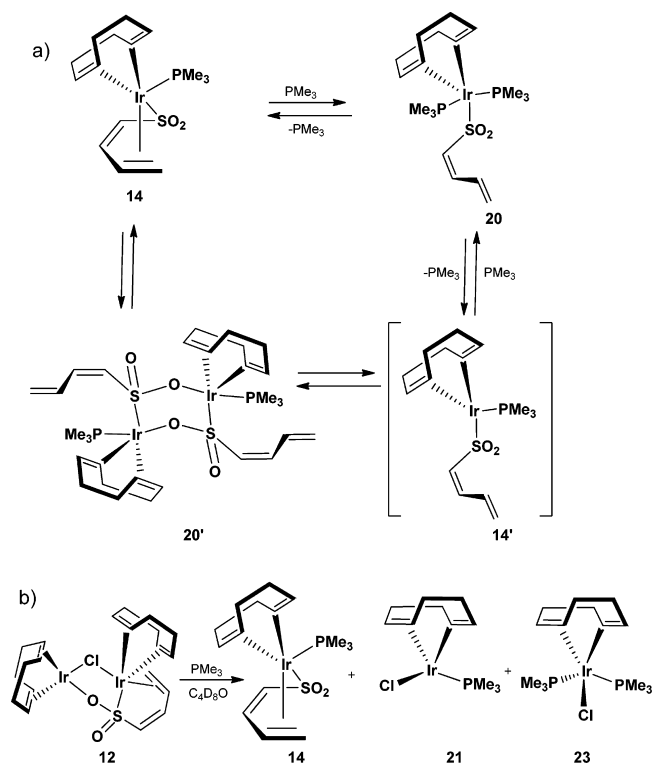
Scheme 6



Compound **19** in the presence of THF and 1.5 equivalents of PMe_3 shows total conversion to a mixture of **14** and **20**, which confirms the lability of the CO – Ir bond, the stronger Ir – PMe_3 bond to give **14**, and the labile coordination of the terminal double bond to afford **20** with two PMe_3 's coordinated to Ir .

The mixture of reaction of **14** and **20** was impossible to purify due to the presence of an equilibria; see Scheme 7a. The low yield obtained for **14** (32%) motivated us to find a better synthetic precursor that did not require the addition of PMe_3 . The complex $[(\eta^4\text{-COD})\text{IrCl}(\text{PMe}_3)_2]$ (**21**) was prepared in 73% yield, which after the metathesis reaction with 3K afforded the corresponding **14**, in 79% yield. Contrasting this result, when $[(\eta^4\text{-COD})\text{IrCl}(\text{PPh}_3)_2]$ (**22**) reacted with 3K , no synthetic

Scheme 7



advantage was found in the formation of **17**, which was isolated in 53.0% yield compared to the 82.0% yield obtained from the addition reaction of PPh_3 to **11**, Scheme 5.

Interestingly, compound $[(\eta^4\text{-COD})\text{IrCl}(\text{PMe}_3)_2]$ (**23**) in the presence of 3K showed, through the ^1H NMR, that it was not a useful precursor of **20** due to its competition in the formation of **14** and an intermediate species, tentatively proposed as $[(\eta^4\text{-COD})\text{Ir}(5\text{-}\eta\text{-SO}_2\text{CHCHCH}_2)(\text{PMe}_3)]_2$ (**20'**),³⁸ which will be discussed below. The reaction between $[(\eta^4\text{-COD})\text{Ir}(\text{PMe}_3)_3]\text{Cl}$ (**24**) and one equivalent of 3K in THF did not show formation of **20** or **20'**, while OPMe_3 , **14**, and an unidentified compound (^{31}P NMR δ –33.0) were detected in 0.14:0.64:0.22 ratio, respectively. According to these results, several monitoring reactions were carried out in order to understand the competition among species present in solution: (a) Reaction between **23** and different stoichiometries of 3K in THF showed that under low concentration of 3K , **14** and small amounts of **20'** were formed, whereas in a 10-fold excess of 3K , compound **20** was also observed, along with **14**, **20'**, **23**, and OPMe_3 . Independently of the concentration of 3K , all reactions favored the formation of **14**.

(b) The reaction between **11** and PMe_3 in $\text{THF-}d_8$, at room temperature, showed basically formation of **14**. A second and third equivalent of PMe_3 showed **20'**, **20**, and **14** in relative 0.43:0.32:0.19 and 0.18:0.58:0.10 ratios, respectively. Even under the presence of free PMe_3 compounds **20'** and **14** remained with **20** in the reaction mixture, which suggests that there is an equilibrium among them (Scheme 7a), as it was also concluded from monitoring the reaction between **12** and PMe_3 (Scheme 7b, *vide infra*).

(c) Compound **12**, in the presence of one equivalent of PMe_3 , in $\text{THF-}d_8$, showed easy coordination and dissociation of the phosphine, which afforded a mixture of **14**, **21**, and **23**, Scheme 7b. First, **23** was predominating, and with time one

PMe₃ was dissociated and **21** and **14** were observed as major compounds in an almost 1:1 ratio. Addition of a second and third equivalent of PMe₃ showed the same trend. As expected, after consecutive addition of two equivalents of **3K**, compound **14** was predominating, and finally, the addition of three more equivalents of PMe₃ gave spectroscopic evidence of **20'** and, in higher amount, compound **20**,³⁹ but always with **14** and free PMe₃.

(d) The reaction of **14** with 1 equiv of PMe₃ in C₆D₆ at room temperature showed immediate transformation into **20** and **20'**, along with **14** and free PMe₃ (Scheme 7a). The addition of two more equivalents of PMe₃ showed the highest amount of **20** formed, along with reduction of the amount of **20'**, **14**, and PMe₃ in a 0.46:0.20:0.04:0.30 ratio, respectively. After 3 days, **20** dissociated with the corresponding increase of **20'**, **14**, and PMe₃ (0.26:0.34:0.07:0.33). From this result, it was also evident that **20** dissociates PMe₃ and the dimer **20'** plays a role in the equilibrium among **14** and **20**. From monitoring reactions b, c, and d, it can be concluded that the excess of PMe₃ favors the formation of **20**, which easily dissociates PMe₃ to afford the coordinatively unsaturated complex (η^4 -COD)Ir(*S*- η -SO₂CHCHCHCH₂)(PMe₃) (**14'**), which can dimerize to **20'** or go back, in the presence of PMe₃, to the formation of **20**. Compound **20'** can also go back to **14**, by dissociation of the dimer and the consequent coordination of the terminal double bond; the presence of this equilibrium avoided a selective reaction for **20**. An even greater lack of selectivity for **20** was observed when iridium chloro complexes, such as **23** or **24**, were used as precursors. According to the reactivity of **21**, **20**, or **23**, it is evident that one Ir–PMe₃ bond bonds strongly, while the second one, in **20** and **23**, is labile.

Considering that the ¹H and ¹³C NMR showed signals for **20'** corresponding to η^4 -COD, *S*- η -SO₂CHCHCHCH₂, and PMe₃, and in order to explain the general trends observed through the monitoring reactions described above, it is being proposed that **20'** is dimeric. It was noted that **20'** was not immediately consumed after being formed, even in excess PMe₃. This fact should discriminate a coordinatively unsaturated complex **14'**, therefore suggesting the tentative formation of a dimeric structure that could be interacting through the S and O atoms of the butadienesulfonyl ligands with the two iridium centers. The S, O-bonded sulfinato complex **20'** is proposed as the kinetic product, while the thermodynamic **20** or **14** is exclusively an S-bound sulfinate, as expected for a soft metal.

Infrared Spectra. The infrared data of the complexes **14**–**19** show several characteristic items connected basically with the sulfoxide group. Strong intensity signals are observed for the antisymmetric and symmetric vibration S=O in the region (1174–1166 and 1110–1098 cm⁻¹) and (1052–1019 cm⁻¹), respectively. Similar stretching frequencies at 1198 (ν_{as}), 1185 (ν_{as}), and 1048 (ν_s) cm⁻¹⁴⁰ are reported for IrCl(CO)-(PPh₃)₂SO₂, where the corresponding bands are at slightly high frequency, which reflects the influence of the butadiene fragment bonded to SO₂, in the case of **14**–**19**. The free SO₂ shows two bands at higher frequencies [1340 (ν_{as}) and 1150 (ν_s) cm⁻¹],⁴⁰ and theoretical and experimental studies related to the vibration of the S=O group,⁴¹ as well as the influence of different solvents in the IR of DMSO and DMSO-*d*₆, have been reported in the region of 1250–1100 cm⁻¹ for ν_{as} and 1100–1000 cm⁻¹ for ν_s .⁴² According to the above, qualitatively, the relative bond order in the S=O bond decreases in the following order: SO₂ > IrCl(CO)(PPh₃)₂SO₂ > **14**–**19** > **12** ~

11 > **10**. Considering the stretching frequencies of other complexes with the butadienesulfonyl ligand, such as the ion-pair complexes Cp**Rh*Cl(*S*- η -SO₂CHCHCHCH₂)(*S*- η -S(O₂⁻K⁺)CHCHCHCH₂) (1175, 1111, and 1050 cm⁻¹)³⁵ and Cp**Ru*(1-2,*S*- η -SO₂CHCHCHCH₂)(*S*- η -S(O₂⁻K⁺)CHCHCHCH₂) (1136, 1108, and 1024 cm⁻¹),³⁴ those could be included in the previous trend, along with complexes **14**–**19** and **10**, respectively, showing better delocalization of the ruthenium complex compared to the isoelectronic rhodium analogue.

The carbonyl stretching frequency in compound **19** shows a strong band at 2049 cm⁻¹, which reflects the lowest retrodonation compared to the thiapentadienyl complex Ir(1-2,*S*- η -CH₂CHCHCHS)(CO)(PPh₃)₂ (**8**) (ν CO, 1982 cm⁻¹), IrCl(CO)(PPh₃)₂ (ν CO, 1954 cm⁻¹), and IrCl(CO)-(PPh₃)₂SO₂ [ν CO, 2013 cm⁻¹; ν SO₂, 1197, 1049 cm⁻¹]⁴³ and (ν CO, 2020 cm⁻¹; ν SO₂, 1198, 1185, 1048, 559 cm⁻¹)⁴⁴.

The carbonyl retrodonation decreases strongly in the presence of the thiapentadienyl ligand, and even more if the sulfonyl or butadienesulfonyl ligand is present, which reflects the π -bonding of SO₂ and consequent lability of CO in the presence of coordinated sulfonyl groups. The fragile bond Ir–CO was also confirmed when **19**, under very mild conditions, afforded a mixture of compounds **14** and **20** (*vide supra*).

NMR Spectra. The presence of the butadienesulfonyl ligand in the complexes **14**–**19** induced a total asymmetry, which was reflected in complex spectra, from which full assignment was done based on two-dimensional HETCOR (¹H, ¹³C) and COSY (¹H, ¹H) experiments, which aided in assigning some of the ¹H and ¹³C signals in Tables 3 and 4, respectively.

There was a preferred coordination mode in the chemistry of the adducts **14**–**19**, where the butadienesulfonyl ligand was coordinated through the sulfur atom η^1 and η^2 with the terminal double bond (C1–C2) to the iridium atom. This type of bonding has been previously observed for several butadienesulfonyl iridium^{15,16} and rhodium^{16,35} compounds, as well as for thiapentadienyl and sulfinylpentadienyl compounds, *vide supra*.

In the ¹³C NMR there was a clear trend of increasing π -retrodonation at C1–C2 going from [(η^4 -COD)Ir(1-2,*S*- η -SO₂CHCHCHCH₂)(PR₃)], where PR₃ increased methyl substitution from PPh₃ until PMe₃, which was also reflected in H1, H1', and H2 through the ¹H NMR.

The cyclooctadiene bound to iridium in **14**–**19** showed eight different carbon atoms, where significant lower frequency chemical shifts were observed for C5 and C6, compared to those of C9 and C10 ($\Delta\delta \cong 20$ – 30), where C9 and C10 showed a significant reduced capability of retrodonation. The coordinated olefins C5–C6 with the strongest and lowest retrodonation were those corresponding to the PMe₃ [C5 (δ 66.38) and C6 (δ 68.16)] and CO [C5 (δ 75.69) and C6 (δ 76.49)] derivatives, respectively.

The ¹H NMR spectra of the COD-coordinated ligand for compounds **14**–**18**, except in a few cases of overlapping, showed nonequivalent hydrogens for the CH and CH₂ signals, which gave evidence for the lack of symmetry of this nonconjugated unsaturated ligand. Full inequivalence of 12 hydrogens of the COD ligand was found in compound **19**, as described in the Supporting Information.

There was significant similarity in the ¹³C chemical shifts of **18** (CDCl₃), **12**, **10**, and **11** (DMSO-*d*₆), which suggests the stronger σ -donor character of DMSO compared to phosphines and CO. The ¹H and ¹³C NMR of compound **18** showed two

magnetically nonequivalent methyl groups for the DMSO ligand (^1H δ : 3.34 and 3.46; ^{13}C δ : 45.49 and 47.10, respectively), which gave evidence of the rigidity and chirality of **18**. Different methyl environments in coordinated DMSO have also been proved as indicative of a lack of any symmetry element in complex $[\text{RuCl}(\text{DMSO})_2\{\text{HB}(\text{methimazolyl})_3\}]$; 45 diastereotopic methyl groups of two equivalent DMSOs *trans* to Cl in $[\text{cis}/\text{fac}-\text{RuCl}_2(\text{DMSO}-\text{O})_3(\text{NO})]\text{BF}_4$ 46 have been reported as well as chiral iridium compounds, such as cyclometalated derivatives of $\text{Cp}^*\text{IrCl}_2(\text{DMSO})$ with crotonic acids 47 or complexes $[\text{Cp}^*\text{IrMe}(\text{DMSO})(\text{X})]$ ($\text{X} = \text{Cl}, \text{Br}, \text{I}$) 48 or $[\text{Cp}^*\text{IrMe}(\text{DMSO})(\text{L})]\text{PF}_6$ ($\text{L} = \text{MeCN}, \text{O}_2\text{CCF}_3$). 48

The ^1H and ^{13}C NMR of **20** are diagnostic and showed that both double bonds of the butadienesulfonyl ligand were not coordinated to the metal. At room temperature, the ^{31}P NMR spectrum of **20** exhibited a singlet at -52.4 ppm. A dynamic process was evident by ^1H and ^{13}C NMR where only one set of CH [3.20 (s); 68.60 (d, 5.3 Hz)], two sets of CH_2 [2.23 (m), 2.40 (m)], and one set of CH_2 [34.18 (s, br)] were observed for the COD-coordinated ligand. There was a typical second-order coupling for the methyl groups of the phosphine ligands in the ^1H NMR (1.62 ppm) and a complex coupling at 20.02 ppm that was observed by ^{13}C NMR. As the ^{31}P NMR of compound **20** ($\delta -52.4$) was identical to **23** or **24** (in CDCl_3 , there was no evidence of dissociation of PMe_3 for **24**), it was only possible to identify **20** by ^1H and ^{13}C NMR. The full spectroscopic NMR data of **22** and **23** are included in Tables 3 and 4 because they have been only partially reported. In **21** and **22** the cyclooctadiene is bound to the square-planar iridium center, showing inequivalent alkene resonances because of the distinct *trans* ligands, as shown by two ^1H NMR signals at lowest field at δ 2.87, 5.33 and δ 2.73, 5.19, for hydrogens of the CH carbons at C5,6 and C9,10, respectively. Those hydrogen signals correlated in the HETCOR (^1H , ^{13}C) spectra with carbon singlets at δ 51.37 and 54.03 and two doublets at δ 93.38 and 94.44 with J_{CP} coupling constant of 14.6 and 14.3 Hz, respectively. The latter coupling reflects the coordination of the corresponding phosphine *trans* to the C9–C10. The trend observed by Crabtree and Morris, 49 concerning the electronic effects of the *trans* ligands in the COD vinyl protons of $[(\eta^4\text{-COD})\text{IrCIL}]$ complexes, was still confirmed for compound **21**. Two pair of carbon signals at δ 33.95, 29.20 and δ 33.90, 29.97 were observed for the methylene carbons in **21** and **22**, from which selective irradiations in **22** and correlation experiments allowed us to assign the corresponding hydrogens C7, C12 and C8, C11 at low and high frequency, respectively.

Crystal Structures. The solid-state structures of compounds **14**, **15**, and **17–20** are presented in Figures 4, 5, and 6–9, respectively. The crystal data and selected bond lengths and angles are provided in Tables 5, 6, and 7, respectively. The crystal structure determination of compound **19** revealed the presence of two independent molecules in the unit cell. These molecules are structurally identical, and for clarity, the crystal data and structure of only one is shown in Tables 5–7 and Figure 8. One and two molecules of chloroform and dichloromethane cocrystallized with compounds **17** and **18**, respectively. Distorted trigonal-bipyramidal (tbp) geometries were established for all crystalline structures. In general, the structural parameters for complexes **14**, **15**, and **17–19** correspond fairly closely to each other. The equatorial plane of the tbp contains the coordinated double bonds C5–C6 of the COD and C1–C2 of the butadienesulfonyl ligands, as well as the P, S, or C atom corresponding to ligand L ($\text{L} =$

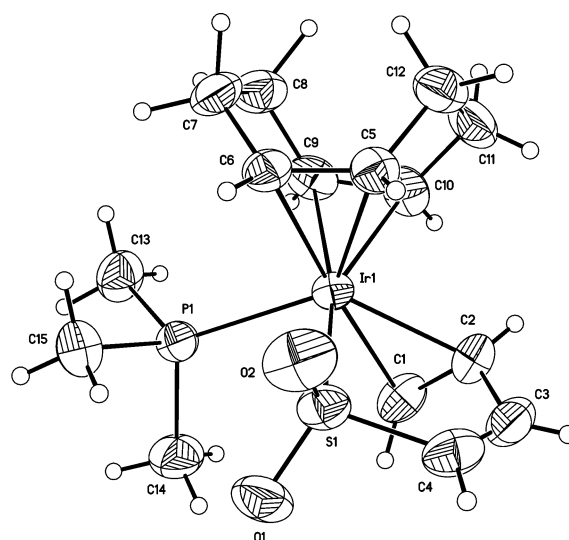


Figure 4. Molecular structure of $(\eta^4\text{-COD})\text{Ir}(1\text{-}2,5\text{-}\eta\text{-CH}_2\text{CHCHCHSO}_2)\text{PMe}_3$ (**14**).

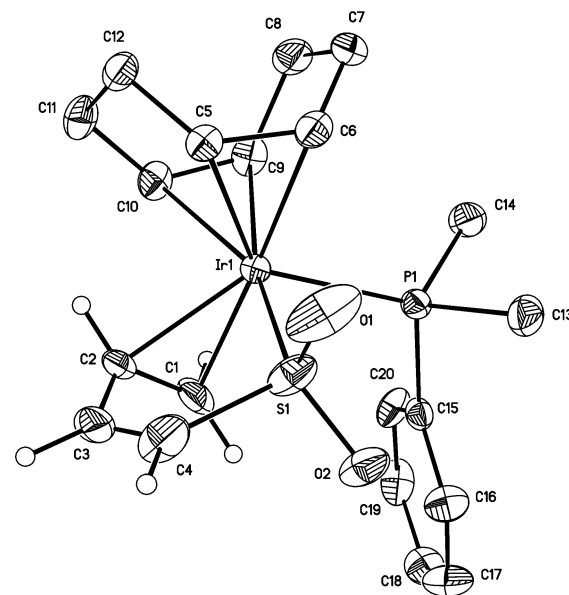


Figure 5. Molecular structure of $(\eta^4\text{-COD})\text{Ir}(1\text{-}2,5\text{-}\eta\text{-CH}_2\text{CHCHCHSO}_2)\text{PMe}_2\text{Ph}$ (**15**). Some hydrogen atoms are omitted for clarity.

phosphine, DMSO, or CO), while the sulfur of the butadienesulfonyl ligand and the double bond C9–C10 of the COD are in axial positions.

The bonding parameters within the butadienesulfonyl ligands are quite similar, except for **20**, which is coordinated exclusively through the sulfur atom. The terminal double bond of the butadienesulfonyl ligands in **14**, **15**, and **17–19** is coordinated to the iridium center, which is clearly demonstrated by the enlargement of the bond lengths due to the retrodonation of C1–C2, which are in the range 1.415–1.434 Å. In contrast, the internal double bonds, which are not coordinated, show the typical sp^2 C3–C4 bond length between 1.293 and 1.340 Å, respectively. The C1–C2–C3–C4 and C2–C3–C4–S1 torsional angles for the (1-2,5- η)-butadienesulfonyl complexes [63.32(1.16)°, 2.43(1.26)° **14**; 63.06(0.69)°, 1.44(0.74)° **15**; 63.49(0.95)°, 5.27(0.97)° **17**; 67.53(1.17)°, 3.63(1.26)° **18**; 61.56(1.03)°, 5.39(1.08)° **19**] imply that the ligand can be

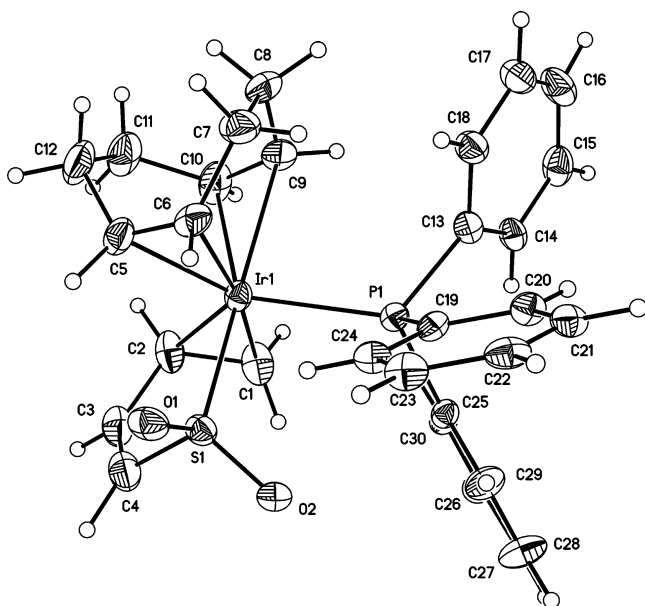


Figure 6. Molecular structure of $(\eta^4\text{-COD})\text{Ir}(1\text{-}2,5\text{-}\eta\text{-CH}_2\text{CHCHCHSO}_2)\text{PPh}_3$ (**17**).

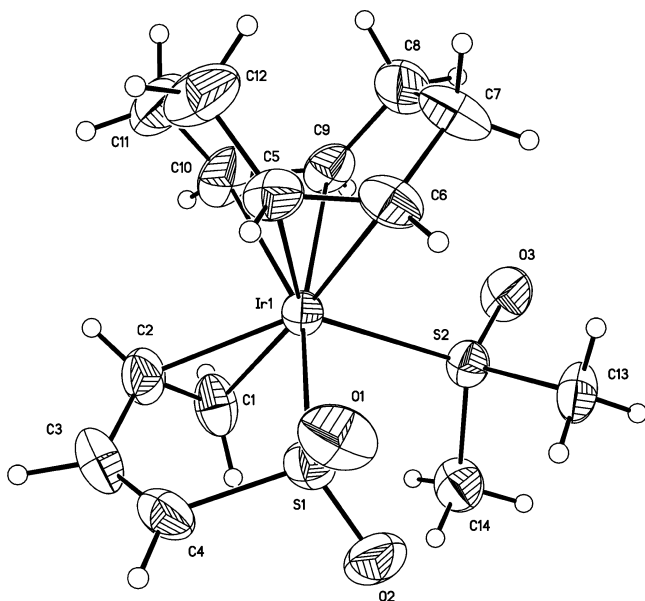


Figure 7. Molecular structure of $(\eta^4\text{-COD})\text{Ir}(1\text{-}2,5\text{-}\eta\text{-CH}_2\text{CHCHCHSO}_2)(\text{DMSO})$ (**18**).

described more accurately as a U conformer than an S one. In contrast, compound **20** shows a torsional angle of $178.55(0.82)^\circ$, $-3.55(1.20)^\circ$, which gives evidence of the butadienesulfonyl ligand being S shaped, and where the double bonds are not coordinated to the iridium atom, according to C1–C2 [1.335(11) Å] and C3–C4 [1.330(9) Å] bond lengths. The C4–S bond length in all crystalline structures reported here showed a carbon bond length that lies between normal C–S single bond (1.82 Å) and double bond (1.60 Å).⁵⁰ Compound **20** [1.790(7) Å] showed the longest C4–S bond lengths, where the coordination of the butadienesulfonyl ligand is through an η^1 -bonding mode. The longer bond distance C4–S observed in **17** [1.788(7) Å] is attributed to the bulky PPh₃ coordinated also to the iridium center.

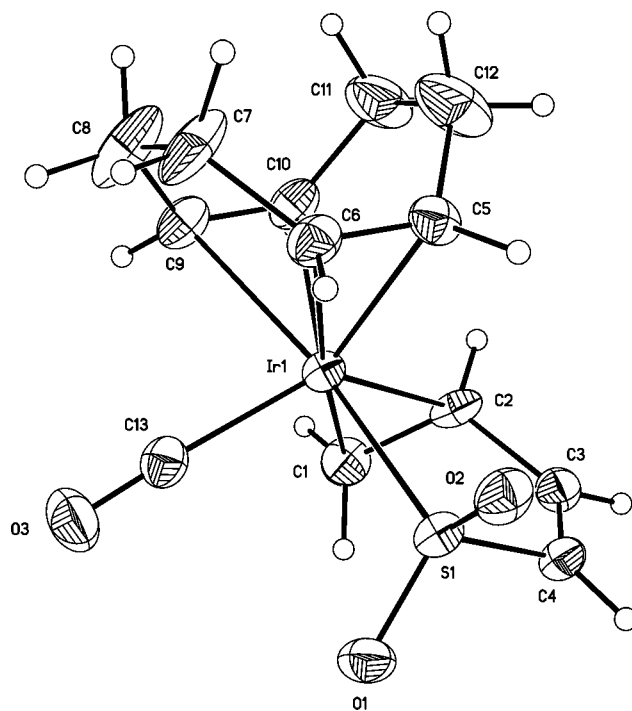


Figure 8. Molecular structure of $(\eta^4\text{-COD})\text{Ir}(1\text{-}2,5\text{-}\eta\text{-CH}_2\text{CHCHCHSO}_2)(\text{CO})$ (**19**).

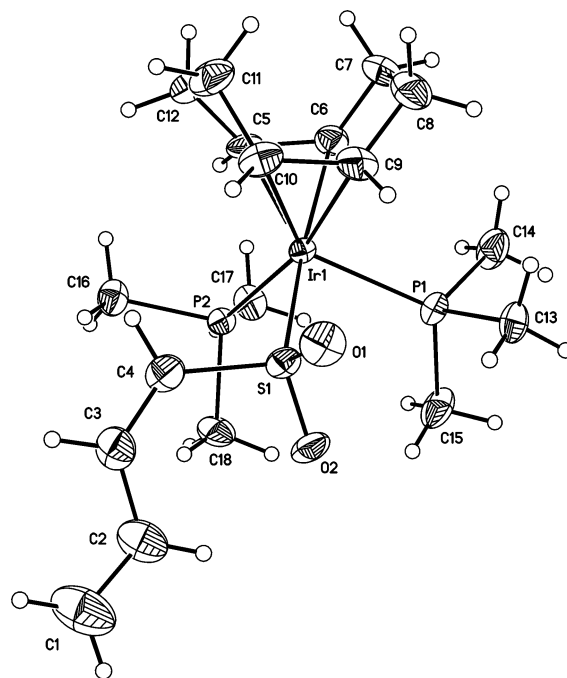


Figure 9. Molecular structure of $(\eta^4\text{-COD})\text{Ir}(5\text{-}\eta\text{-CH}_2\text{CHCHCHSO}_2)(\text{PMe}_3)_2$ (**20**).

The S1–O1 and S1–O2 (average value 1.46 Å) reflect typical values for sulfonyl groups (1.457 Å).⁵¹ The Ir–S bond lengths decreased according to the number of oxygen atoms bonded to sulfur, as observed in **5** [2.3788(18), 2.4900(17) Å], **9** [2.329(2), 2.444(3) Å], and the average value of 2.31 Å found in butadienesulfonyl derivatives **14**, **15**, and **16–19**. The Ir–P bond lengths showed, as expected, the longest value for the bulky triphenylphosphine complex **17** [2.4563(16) Å], and **20** showed different Ir–P bond lengths [Ir1–P1, 2.3731(14) and

Table 7. Selected Bond Angles (deg) for Compounds 12, 14, 15, and 17–20

	12	14	15	17	18	19	20
C(1)–C(2)–C(3)	119.0(6)	117.4(8)	120.9(4)	117.8(7)	119.7(9)	117.6(6)	122.3(9)
C(2)–C(3)–C(4)	122.3(6)	123.2(8)	122.9(4)	123.4(7)	121.1(7)	121.8(6)	130.0(7)
C(3)–C(4)–S(1)	117.2(5)	117.4(7)	118.0(4)	116.8(6)	117.6(6)	117.9(5)	128.6(5)
C(4)–S(1)–Ir(1)	103.2(2)	102.6(3)	101.9(2)	102.4(3)	102.7(3)	103.1(2)	108.6(2)
C(1)–Ir(1)–S(1)	92.57(18)	88.1(2)	89.23(14)	88.6(2)	90.6(3)	91.54(18)	85.75(18)
C(2)–Ir(1)–S(1)	82.75(17)	81.7(2)	81.58(13)	81.9(2)	81.5(2)	82.12(16)	89.40(17)
C(5)–Ir(1)–S(1)	88.15(18)	89.2(2)	87.85(11)	88.62(19)	89.2(2)	89.40(17)	90.47(17)
C(6)–Ir(1)–S(1)	92.86(17)	91.3(2)	90.37(12)	90.43(16)	91.4(2)	92.48(17)	90.47(17)
C(9)–Ir(1)–S(1)	164.28(17)	167.8(2)	167.73(12)	166.37(19)	167.8(2)	165.41(17)	169.71(17)
C(10)–Ir(1)–S(1)	158.94(17)	154.1(2)	152.62(12)	154.72(19)	154.1(2)	158.08(18)	146.76(16)
Ir(1)–S(1)–O(1)	116.5(2)	113.1(2)	113.12(15)	113.58(19)	113.9(3)	113.34(19)	112.5(2)
Ir(1)–S(1)–O(2)	115.71(19)	116.1(3)	116.88(14)	115.73(18)	114.0(3)	113.48(19)	113.67(18)
C(1)–Ir(1)–C(5)	137.9(3)	137.6(3)	139.14(15)	132.2(3)	139.4(3)	135.3(3)	128.90(19)
C(1)–Ir(1)–C(6)	173.5(2)	175.9(3)	177.30(17)	170.6(3)	176.3(3)	171.6(3)	167.21(18)
C(1)–Ir(1)–C(9)	95.7(3)	102.3(3)	101.95(18)	104.3(3)	100.1(3)	99.1(2)	99.88(17)
C(1)–Ir(1)–C(10)	86.6(3)	85.4(3)	86.23(18)	84.6(3)	84.5(4)	85.1(3)	79.29(16)
C(2)–Ir(1)–C(5)	100.0(3)	99.2(3)	100.83(16)	94.2(3)	101.6(3)	98.0(3)	90.39(5)
C(2)–Ir(1)–C(6)	138.8(3)	137.3(3)	138.74(16)	132.4(3)	138.9(4)	135.3(3)	98.34(5)
C(2)–Ir(1)–C(9)	111.9(2)	110.5(3)	110.32(17)	110.9(3)	110.6(3)	112.4(2)	98.34(5)
C(2)–Ir(1)–C(10)	83.5(2)	77.6(3)	78.09(17)	77.7(3)	78.9(4)	81.9(2)	81.9(2)
C(1)–Ir(1)–C(2)	38.7(3)	38.6(3)	38.56(16)	38.3(3)	38.4(3)	38.3(2)	38.3(2)
C(9)–Ir(1)–P(1)	108.33(5)	84.7(2)	84.66(12)	85.32(18)	130.0(3)	130.0(3)	89.69(16)
C(10)–Ir(1)–P(1)	115.71(19)	117.2(2)	116.87(12)	114.39(19)	91.86(7)	91.86(7)	123.09(16)
P(1)–Ir(1)–S(1)	132.9(3)	88.26(8)	90.17(4)	90.05(5)	92.7(2)	92.7(2)	89.47(5)
C(5)–Ir(1)–P(1)	134.32(18)	128.2(2)	129.74(10)	136.15(19)			132.47(19)
C(6)–Ir(1)–P(1)	91.12(18)	90.0(2)	91.67(12)	97.8(2)			94.42(18)
C(1)–Ir(1)–P(1)	166.6(3)	94.0(2)	91.00(12)	91.52(19)			
	89.84(12)			166.37(19)			
	O(2)–Ir(2)–Cl(2)			S(1)–Ir(1)–C(9)			

Ir1–P2, 2.3334(13) Å], where the shortest is reflecting a higher *trans* effect of the COD ligand on P2.

The iridium–COD bonding in **14**, **15**, and **17–19** showed, as expected for d^8 t_{2g} geometry,⁵² shorter Ir–C bond lengths for the equatorial Ir–C5 [range: 2.169–2.203 Å] and Ir–C6 [range: 2.170–2.198 Å] compared to the axially coordinated Ir–C9 [range: 2.280–2.329 Å] and Ir–C10 [range: 2.249–2.287 Å], which confirms the strongest binding of an olefin to a d^8 metal center in a trigonal plane. This stronger iridium–olefin interaction is also reflected in the longer bond length between C5–C6 [range: 1.401–1.434 Å], which gives evidence of a more efficient retrodonation compared to that of C9–C10 [range: 1.372–1.390 Å].

Compound **20** showed a similar trend; however, the differences between Ir–C of the corresponding C5 [2.190(6) Å], C6 [2.168(5) Å] and C9 [2.200(6) Å], C10 [2.229(5) Å] were shorter. The bond lengths C5–C6 [1.437(9) Å] and C9–C10 [1.412(9) Å] were slightly different from those described before; this seems to be the result of the presence a second phosphine P2, C6–Ir–P2 [167.21(18)°], where a *trans* influence was also present. A more symmetric coordination of the cyclooctadiene ligand was also observed through NMR spectroscopy in solution for **20**.

Comparison of the bond lengths of C1–C2 of the phosphine derivatives **14** [1.426(12) Å], **15** [1.434(6) Å], and **17** [1.429(10) Å] with the corresponding Ir(2,4-dimethyl-1,4-5- η -pentadienyl)(PMe₃)₃ [1.469(13) Å]³¹ shows a lower retrodonation in the butadienesulfonyl derivatives, as expected for less electron-rich complexes. A higher retrodonation of the cyclooctadiene ligand in the thiapentadienyl **5** related to 1-2,5- η -butadienesulfonyl derivatives **14–19** (independently of the substituted L) was observed, according to longer carbon–carbon double bond lengths [C5–C6, 1.446(12) Å and C9–C10, 1.403(12) Å] and shorter carbon–iridium bond lengths [C5–Ir, 2.135(7) Å; C6–Ir, 2.155(8) Å; C9–Ir, 2.182(8) Å; C10–Ir, 2.201(8) Å] compared to those of 1-2,5- η -butadienesulfonyl derivatives [C5–C6, range: 1.401–1.426 Å, except for **17** (1.434(10) Å); C9–C10, range: 1.372–1.390 Å; C5–Ir, range: 2.169–2.203 Å; C6–Ir, range: 2.170–2.198 Å; C9–Ir, range: 2.243–2.329 Å; C10–Ir, range: 2.249–2.287 Å]. A similar trend was observed for **22** and **17**, in which **22** showed a better retrodonation, in a more symmetric cyclooctadiene–iridium interaction, according to carbon–carbon and carbon–iridium bond lengths.⁵³ The Ir–P bond length is strongly affected by the presence of the sulfonyl group in the heterodienyl ligand, as observed from **14** [2.398(2) Å] and **20** [2.3731(14) Å], which show significantly longer Ir–P bond lengths compared to those of thiapentadienyl and pentadienyl derivatives: Ir(1-2,5- η -thiapentadienyl)(PMe₃)₃ [2.261(3), 2.293(3), and 2.323(2) Å]⁴ and Ir(2,4-dimethyl-1,4-5- η -pentadienyl)(PMe₃)₃ [2.291(3), 2.288(2), and 2.323(3) Å].³¹ Similarly long bond values were found for butadienesulfonyl derivatives with PMe₂Ph [2.3896(10) Å, **15**] and PPh₃ [2.4563(16) Å, **17**]. Also, the Ir–S, Ir–C1, and Ir–C2 showed clearly the influence of the sulfonyl group. The Ir–S bond lengths in compounds **14**, **15**, **17**, **18**, **19**, and **20** are shorter (range: 2.3011–2.3168 Å) compared to those of the thiapentadienyl complex Ir(1-2,5- η -thiapentadienyl)(PMe₃)₃ [2.417(3) Å],⁴ while Ir–C1 (range: 2.140–2.177 Å) and Ir–C2 (range: 2.163–2.191 Å) are longer compared to those of the thiapentadienyl complex [2.110(9) and 2.139(9) Å],⁴ respectively. Comparison of [Cp*Ir(PMe₃)(SO₂Me)(MeCN)]-[OTf]⁵⁴ shows shorter and longer bond lengths for Ir–P

[2.317(3) Å] and Ir–S [2.334(3) Å], respectively, than those observed in **14** [Ir–P, 2.398(2) Å; Ir–S, 2.3076(19) Å].

A comparison with pentadienyl complexes, such as Ir(2,4-dimethyl-1,4-5- η -pentadienyl)(CO)(PPh₃)₂³¹ and Ir(*syn*-1-3- η -pentadienyl)(CO)(PPh₃)₂,³¹ was carried out due to the lack of crystalline structures of iridium complexes that contain thiapentadienyl, along with CO and/or PPh₃ ligands. The Ir–P is significantly longer for **17** [2.4563(16) Å] compared to Ir(2,4-dimethyl-1,4-5- η -pentadienyl)(CO)(PPh₃)₂ [2.336(2) Å] and Ir(*syn*-1-3- η -pentadienyl)(CO)(PPh₃)₂ [2.296(3) Å], while bond angles P1–Ir1–C1 are very close to 90° in all cases. The Ir–CO bond length is significantly longer in **19** [1.950(7) Å] compared to pentadienyl complexes described above: 2,4-dimethyl derivative [1.886(7) Å] and *syn*-1-3- η -pentadienyl [1.872(12) Å]. The same trend was reflected through the IR spectra, *vide supra*.

CONCLUSIONS

This study demonstrates that the thiapentadienyl, sulfinylpentadienyl, and butadienesulfonyl in cyclooctadiene iridium complexes can act as sulfur and oxygen bridging ligands. Compounds **5**, **6**, and **10–19** show totally asymmetric cyclooctadiene ligands. The presence of the SO₂ in the heterodienyl ligand modifies significantly the structural and electronic properties of the corresponding metallic derivatives, compared to those previously obtained with the oxo, aza, and thiapentadienyl ligands. The research in the field of butadienesulfonyl ligands will continue in order to explore and learn, in more detail, about their synthetic potential; this will afford novel properties, such as bonding mode, polarity, chirality, and peculiar reactivity.

EXPERIMENTAL SECTION

All experiments were carried out under a nitrogen atmosphere by using standard Schlenk-type equipment, and the hydrides and lithium and potassium salts were weighed in a glovebox. The solvents were dried by standard methods (diethyl ether and THF with Na/benzophenone) and distilled under nitrogen prior to use. Deuterated solvents were degassed, and DMSO-*d*₆ (Cambridge Isotopes Laboratory Inc.) was dried with Na before use. The preparation of sodium and potassium thiapentadienyl salts^{17,19} **1Na**, **1K**, and sulfinylpentadienyl **2K**¹⁹ and lithium and potassium butadienesulfonyls **3Li**, **3K**, and Li[MeCHCHC(Me)CHSO₂]₂¹⁹ as well as complexes [Ir(η^4 -COD)(μ -Cl)]₂ (**4**),⁵⁵ *trans*-Ir(CO)Cl(PPh₃)₂ (**7**),^{56,57} Ir(η^4 -COD)Cl(PPh₃)₂ (**22**),^{49,53,58} Ir(η^4 -COD)Cl(PMe₃)₂ (**23**),⁵⁷ and [Ir(η^4 -COD)(PMe₃)₃]Cl (**24**)⁵⁹ has already been published. All other chemicals were used as purchased from Pressure Chemicals, Sigma-Aldrich, Strem Chemicals, Merck, and J. T. Baker, Co. (industrial grade).

The ¹H, ¹³C, ³¹P, ⁷Li, and ¹¹B NMR spectra were recorded on Bruker 300, Jeol GSX-270, and JEOL Eclipse 400 MHz instruments and referenced internally using the residual protio and carbon solvent resonances relative to tetramethylsilane. External standards for ³¹P and ⁷Li NMR were H₃PO₄ and LiCl. Mass spectra were recorded on a Hewlett-Packard 5890-MS-Engine. High-resolution mass spectra were obtained by LC/MSD TOF on an Agilent Technologies instrument with APCI as ionization source and FAB or ESI at the University of Washington, St. Louis, MO, USA. Elemental analyses were performed in a Thermo-Finnigan model Flash 1112 at the Chemistry Department at Cinvestav and Desert Analytics, Tucson, AZ, USA. Infrared spectra were recorded on a FT-IR Perkin-Elmer 1600 spectrometer using KBr pellets (4000–400 cm⁻¹) and Nujol in PTFE (4000–200 cm⁻¹). Melting points were determined in a Melt-Temp Gallenkamp (digital) and are uncorrected.

Dynamic Laser-Light Scattering (DLS) Instrumentation and Measurements. For dynamic DLS measurements of compounds **10**,

11, and 17, the samples were prepared in THF at highly diluted concentrations, and then they were filtered through a Millipore 0.5 μm LCR filter for dust removal and poured in a quartz cell. A commercial DLS spectrometer (Malvern Zetasizer Nano 90) equipped with a fast correlator card (minimum sample time is 12.5 ns) and temperature control from 2 to 90 $^{\circ}\text{C}$ was used for measurements. A He–Ne laser operated at 633 nm and 4.0 mW was used as the light source using a multiple narrow method. The primary beam was vertically polarized. Scattered intensity was taken at 90 $^{\circ}$ to the incident beam. For the calculation of the hydrodynamic radius R_h in THF values of 0.4549 and 1.409 were used for the viscosity η and the refractive index RI , respectively. A value of 1.4 was used as the refractive index of complexes 10, 11, and 17.

Crystal Structure Determination. X-ray diffraction measurements were made at 169(2) K (17, 19, 20); 198(2) K (15); 203(2) K (14); and 293(2) K (9, 12, 18) on an Enraf Nonius-Kappa CCD or at 298(2) K on a CAD4 (5) diffractometer, using graphite-monochromated Mo $K\alpha$ radiation ($\lambda = 0.71073 \text{ \AA}$). A summary of crystal data collection and refinement (SHELX-97) parameters for compounds is given in Tables 1, 2, and 5–7. The ellipsoids were drawn at 45% probability for all crystalline structures.

Synthesis of $[(\eta^4\text{-COD})\text{Ir}(1\text{-}2,5\text{-}\eta\text{-}(\mu_2\text{-S})\text{CH}=\text{CHCH}=\text{CH}_2)]_2$ (5). Into a Schlenk flask equipped with a stir bar were placed NaH (12.0 mg, 0.49 mmol), 0.8 mL of DMSO- d_6 , and 2,5-dihydrothiophene (36.3 μL , 39.0 mg, 0.45 mmol). After the mixture was stirred in an ultrasonic bath for 9 h (25–35 $^{\circ}\text{C}$), an amber solution was observed, and 4 (150.0 mg, 0.22 mmol) was added; a brown solid in a dark red solution was obtained immediately. Addition of hexane afforded more brown solid, which was filtered and washed with hexane. The volume of the dark red solution was reduced, and more precipitate was obtained after addition of acetone. The solid was recrystallized from $\text{CH}_2\text{Cl}_2/\text{Et}_2\text{O}$ at 0 $^{\circ}\text{C}$ as a yellow, crystalline solid in 47.1% yield (81.0 mg, 0.105 mmol). Mp: 181–184 $^{\circ}\text{C}$. EI-MS (70 eV): m/z 772 $[\text{M}]^+$, 662, 577, 554, 384, 301, 277, 245. Anal. Calcd for $\text{C}_{24}\text{H}_{34}\text{S}_2\text{Ir}_2$: C 37.39, H 4.44. Found: C 37.70, H 4.47.

Synthesis of $[(\eta^4\text{-COD})\text{Ir}(1\text{-}2,5\text{-}\eta\text{-S}\text{CH}=\text{CHCH}=\text{CH}_2)\text{PMe}_3]$ (6). Compound 5 (58.0 mg, 0.075 mmol) was placed in a Schlenk flask with a stir bar and was dissolved in 10 mL of CH_2Cl_2 . The solution was cooled at –78 $^{\circ}\text{C}$, and PMe_3 (0.018 mL, 0.17 mmol) was added. The reaction mixture was allowed to reach room temperature and was stirred 2 h; the yellow color of the solution faded. The solvent was removed under vacuum, and 6 was extracted from the residue with hexane, affording a yellow solid in 53.2% yield (37.0 mg, 0.08 mmol). Mp: 78–79 $^{\circ}\text{C}$. EI-MS (70 eV): m/z 462 $[\text{M}]^+$, 407, 385, 376, 303, 268, 108, 85, 76, 61, 53.

Synthesis of $[\text{Ir}(1\text{-}2,5\text{-}\eta\text{-S}\text{CH}=\text{CHCH}=\text{CH}_2)(\text{CO})(\text{PPh}_3)_2]$ (8). Compound 7 (300.0 mg, 0.384 mmol) was placed in a Schlenk flask with a stir bar and was dissolved in 15 mL of THF. Slow addition of 0.4 mL of 1K in DMSO (0.24 g/mL, 95.0 mg, 0.77 mmol), at room temperature, afforded an amber solution, which was stirred for 2 h. Removal of the solvent under vacuum gave an oily solid, which was washed with deoxygenated water (4 \times 5 mL) and dried in an oil bath (55 $^{\circ}\text{C}$) under vacuum for 9 h. A cream solid was isolated in 81.8% yield (261.0 mg, 0.32 mmol). Mp: 140–143 $^{\circ}\text{C}$. IR (KBr): 3055 (m), 2336 (w), 1982 (vs), 1572 (m), 1481 (m), 1434 (s), 1307 (w), 1186 (m), 1092 (m), 1028 (w), 999 (w), 988 (w), 848 (w), 746 (m), 696 (s), 515 (s), 453 (w), 418 (w). LR FAB-MS: m/z 830 $[\text{M}]^+$, 745, 715, 636, 568, 540, 453, 375. Anal. Calcd for $\text{C}_{41}\text{H}_{35}\text{OP}_2\text{SiR}_2\text{H}_2\text{O}$: C 58.08, H 4.16. Found: C 58.06, H 4.29.

Synthesis of $[(\eta^4\text{-COD})\text{Ir}(1\text{-}2,5\text{-}\eta\text{-}(\mu\text{-SO})\text{CH}=\text{CHCH}=\text{CH}_2)]_2$ (9). KH (7.0 mg, 0.18 mmol) and 0.8 mL of DMSO- d_6 were placed into a Schlenk flask equipped with a stir bar, and the mixture was cooled at 0 $^{\circ}\text{C}$. A mixture of 0.025 mL of 2,3- and 2,5-dihydrothiophene-1-oxide in 37.5% and 62.5% yield (11 mg, 0.11 mmol and 18.6 mg, 0.18 mmol, respectively) was added. The reaction mixture reached room temperature, and after 30 min of stirring, a green solution was obtained. Addition of 4 (50.0 mg, 0.074 mmol) afforded an amber solution and a green-yellow solid suspension. After 30 min the reaction mixture was filtered and the solid was washed with Et_2O . The solid was treated with CH_2Cl_2 , and a small amount of a

brown solid was removed. Evaporation of the solvent and drying under vacuum afforded 24.0 mg of yellow solid, which after recrystallization in $\text{CH}_2\text{Cl}_2/\text{Et}_2\text{O}$ afforded yellow crystals (5 mg), which did not melt below 260 $^{\circ}\text{C}$.

Synthesis of $[(\eta^4\text{-COD})\text{IrCl}(1\text{-}2,5\text{-}\eta\text{-}(\text{SO}_2\text{Li})\text{CH}=\text{CHCH}=\text{CH}_2)]$ (10). A suspension of 3Li (37.0 mg, 0.30 mmol) in THF (5 mL) was stirred and added dropwise, at –110 $^{\circ}\text{C}$ (liquid N_2/EtOH), to a suspension of 4 (100 mg, 0.15 mmol) in 5 mL of THF. The reaction mixture was allowed to reach room temperature ($\cong 40$ min) and was stirred for an additional 1 h. The amber solution was filtered, and the volume of THF was reduced to $\cong 2$ mL. Addition of diethyl ether ($\cong 12$ mL) gave a precipitate, which, after filtration, washing three times with diethyl ether (4 mL), and subsequent drying, afforded a cream powder of 10 (95.0 mg, 0.021 mmol) in 69.0% yield, which did not melt below 250 $^{\circ}\text{C}$. IR (KBr, cm^{-1}): 1638 (s, br), 1612 (s, br), 1473 (w), 1446 (m), 1429 (sh), 1358 (vw), 1333 (m), 1305 (s), 1248 (w), 1218 (w), 1133 (vs, br), 1108 (vs, sh), 1029 (vs, br), 875 (m), 828 (vs), 784 (w), 733 (s), 669 (s), 571 (s), 448 (s, br). LR FAB-MS (matrix: 3-NBA-Li): m/z 460 $[\text{M}^+]$, 425, 417, 353, 313, 307, 289. HR FAB-MS: m/z 425.0734 (–1.1 ppm). Anal. Calcd for $\text{C}_{12}\text{H}_{17}\text{ClLiO}_2\text{SiR}$: C, 31.34; H, 3.73. Found: C, 31.42; H, 4.18.

Synthesis of $[(\eta^4\text{-COD})\text{IrCl}(1\text{-}2,5\text{-}\eta\text{-}(\text{SO}_2\text{K})\text{CH}=\text{CHCH}=\text{CH}_2)]$ (11). A suspension of 3K (139.5 mg, 0.90 mmol) in THF (10 mL) was stirred and added, dropwise at –110 $^{\circ}\text{C}$ (liquid N_2/EtOH), to a suspension of 4 (300.0 mg, 0.45 mmol) in 20 mL of THF. The reaction mixture was allowed to reach room temperature ($\cong 40$ min) and was stirred for an additional hour. The solution was filtered three times, and the volume of THF was reduced to 5 mL. Addition of pentane (70 mL) allowed the precipitation of a cream powder, which after drying under vacuum, afforded compound 11 in 66.0% yield (270.0 mg, 0.55 mmol). It did not melt up to 250 $^{\circ}\text{C}$. The THF/pentane solution was evaporated under vacuum to afford 12 in 9.0% yield (30.0 mg, 0.04 mmol). Compound 11: IR (KBr, cm^{-1}): 1639 (s, sh), 1611 (s), 1474 (m), 1446 (s), 1358 (w), 1332 (s, sh), 1306 (s), 1217 (w), 1146 (vs, br), 1108 (vs, sh), 1041 (vs, br), 949 (w), 874 (w), 824 (s), 786 (w), 731 (s), 666 (s), 569 (s), 523 (w), 445 (s). IR (Nujol, cm^{-1}): 251 (s), 234 (m). ESI+ TOF: ($\text{C}_{12}\text{H}_{17}\text{O}_2\text{SKIr}$) m/z 457.0210; error ppm: –0.0614; DBE: 5.0. Anal. Calcd for $\text{C}_{12}\text{H}_{17}\text{ClKO}_2\text{SiR}$: C, 29.29; H, 3.48; S, 6.52. Found: C, 29.17; H, 3.88; S, 6.81.

Synthesis of $[(\eta^4\text{-COD})\text{Ir}(\mu\text{-Cl})(1\text{-}2\text{-}\eta\text{-S}\text{O}\text{-}\mu\text{-OSOCH}=\text{CHCH}=\text{CH}_2)]_2$ (12). A suspension of 3K (139.5 mg, 0.90 mmol) in THF (10 mL) was stirred and added dropwise at –110 $^{\circ}\text{C}$ (liquid N_2/EtOH) to a suspension of 4 (300.0 mg, 0.45 mmol) in 20 mL of THF. The reaction mixture was allowed to reach –70 $^{\circ}\text{C}$. The solution was immediately filtered three times at this temperature; the solution was kept in a cold bath, and the volume of THF was reduced to 5 mL. Addition of pentane (70 mL) allowed the precipitation of a cream solid, which, after filtration and drying, afforded compound 11 (76 mg, 0.15 mmol) in 19.0% yield. The cold solution was evaporated under vacuum to afford a crystalline yellow solid in 60.0% yield (200.0 mg, 0.26 mmol). Compound 12 decomposes at 150 $^{\circ}\text{C}$ without melting. Single crystals were obtained from recrystallization of THF/pentane. IR (KBr, cm^{-1}): 1639 (s, br), 1609 (s, br), 1472 (s, sh), 1447 (s), 1380 (w), 1331 (m), 1305 (s), 1266 (vw), 1220 (vw), 1151 (vs, br), 1107 (s, sh), 1034 (vs), 1004 (s, sh), 952 (vs), 915 (w), 872 (w), 828 (s), 785 (w, sh), 726 (s), 664 (s), 592 (w), 568 (w), 522 (vw), 445 (m). IR (Nujol, cm^{-1}): 251 (s). ESI+ TOF: m/z 719.1216 $[\text{M}^+ - \text{Cl}]$. Anal. Calcd for $\text{C}_{20}\text{H}_{29}\text{ClO}_2\text{SiR}_2$: C, 31.89; H, 3.88; S, 4.26. Found: C, 32.04; H, 3.94; S, 3.87.

Synthesis of $[(\eta^4\text{-COD})\text{Ir}(1\text{-}2,5\text{-}\eta\text{-SO}_2\text{CH}=\text{CHCH}=\text{CH}_2)\text{PMe}_3]$ (14). (a) PMe_3 (15.0 mg, 21.0 μL , 0.20 mmol) was added to a yellow solution of 11 (100.0 mg, 0.20 mmol) in THF (20 mL) at –110 $^{\circ}\text{C}$ (liquid N_2/EtOH). After 10 min, the reaction mixture was allowed to reach room temperature and was stirred for an additional hour. The solution was filtered three times, and the volume of THF was reduced to 5 mL. Addition of pentane (60.0 mL) allowed the precipitation of a light yellow powder, which, after drying under vacuum, afforded compound 14 in 32.0% yield (32.0 mg, 0.065 mmol), with mp 199–201 $^{\circ}\text{C}$. Single crystals were obtained from a CHCl_3 solution at –40

$^{\circ}\text{C}$. IR (CDCl_3 , cm^{-1}): 2964 (w), 2845 (w), 2241 (w), 1613 (w), 1415 (w, br), 1261 (s), 1167 (vw), 1098 (s), 1047 (s), 1016 (s), 960 (vw), 919 (vs, sh), 900 (vs), 867 (vw), 808 (s), 754 (s), 716 (s), 651 (s), 561 (vw), 525 (vw). IR (KBr, cm^{-1}): 1638 (w, sh), 1614 (s), 1474 (w), 1455 (w), 1424 (s), 1385 (w), 1359 (w), 1336 (w), 1304 (s), 1281 (s, sh), 1215 (w), 1170 (vs, br), 1098 (s), 1048 (vs, br), 951 (vs, br), 902 (w, sh), 848 (m), 816 (s), 731 (m), 710 (s), 658 (m), 557 (m), 522 (m), 440 (s). EI-MS (20 eV): m/z 494 (2) [M^+], 430, 374, 295, 109. Anal. Calcd for $\text{C}_{13}\text{H}_{26}\text{O}_2\text{PSIr}$: C, 36.50; H, 5.31. Found: C, 36.65; H, 5.33.

(b) Compound **21** (132.0 mg, 0.32 mmol) was dissolved in THF (15 mL) to give an orange solution, which was cooled at $-110\text{ }^{\circ}\text{C}$ (liquid N_2/EtOH); then, **3K** (60.0 mg, 0.38 mmol), previously suspended in THF, was added. The reaction mixture was allowed to reach room temperature and was stirred 1.5 h, and a slightly yellow suspension was obtained. The volume of the solution was reduced to ~ 3 mL under vacuum, and cold hexane (60 mL) was added. A cream solid precipitated, which was filtered and dried to afford 125.0 mg (79.0%, 0.25 mmol).

Synthesis of $[(\eta^4\text{-COD})\text{Ir}(1\text{-}2,5\text{-}\eta\text{-SO}_2\text{CH}=\text{C}(\text{Me})\text{CH}=\text{CHMe})\text{PMe}_3]$ (14Me**).** A suspension of $\text{Li}[\text{SO}_2\text{CHC}(\text{Me})\text{CHCHMe}]$ (23.0 mg, 0.15 mmol) in THF (14 mL) was stirred and added dropwise at $-110\text{ }^{\circ}\text{C}$ (liquid N_2/EtOH) to a suspension of **4** (50.0 mg, 0.074 mmol) in 4 mL of THF. The reaction mixture was allowed to reach room temperature ($\cong 40$ min) and was stirred for an additional 75 min. The amber solution was cooled again to $-110\text{ }^{\circ}\text{C}$, and PMe_3 (11.4 mg, 16.0 μL , 0.15 mmol) was added. The solution reached room temperature and was stirred for 90 min. The yellow solution was filtered, and the volume of THF was reduced to $\cong 2$ mL. Addition of diethyl ether gave a precipitate, which, after filtration, washing with hexane, and subsequent drying, afforded a yellow-cream solid of **14Me** (44.0 mg, 0.084 mmol) in 56.7% yield. IR (CDCl_3 , cm^{-1}): 1603 (vw), 1430 (w, br), 1261 (m), 1156 (m, br), 1098 (m, br), 1042 (s), 1022 (m, sh), 957 (w), 916 (vs, sh), 900 (vs), 866 (vw), 807 (m, br), 754 (vs, br), 722 (vs, br), 651 (s), 613 (vw), 557 (w), 515 (w).

Synthesis of $[(\eta^4\text{-COD})\text{Ir}(1\text{-}2,5\text{-}\eta\text{-SO}_2\text{CH}=\text{CHCH}=\text{CH}_2)\text{PMe}_2\text{Ph}]$ (15**).** This reaction was conducted analogously to method (a) for **14**, using compound **11** (100.0 mg, 0.20 mmol) in 10 mL of THF and PMe_2Ph (28.0 mg, 29.0 μL , 0.20 mmol). Workup was conducted similarly. A pale cream powder of **15** was obtained in 97.0% yield (110.0 mg, 0.20 mmol), with mp $219\text{--}220\text{ }^{\circ}\text{C}$ (dec). Recrystallization ($\text{CH}_2\text{Cl}_2/\text{Et}_2\text{O}$, 1:2) at $-40\text{ }^{\circ}\text{C}$ gave colorless crystals for the X-ray diffraction study. IR (CHCl_3): 1610 (w), 1480 (w), 1439 (m), 1411 (sh), 1384 (w), 1334 (w), 1302 (w), 1262 (vs), 1189 (m), 1169 (m), 1110 (vs), 1019 (vs), 958 (m), 918 (s), 872 (w), 800 (vs), 699 (m, br), 655 (w), 556 (m), 521 (w), 493 (m), 442 (m), 415 (w). EI-MS: m/z 556 [M^+], 492, 435, 330, 138. Anal. Calcd for $\text{C}_{20}\text{H}_{28}\text{O}_2\text{PSIr}$: C, 43.23; H, 5.08. Found: C, 43.53; H, 5.30.

Synthesis of $[(\eta^4\text{-COD})\text{Ir}(1\text{-}2,5\text{-}\eta\text{-SO}_2\text{CH}=\text{CHCH}=\text{CH}_2)\text{PMePh}_2]$ (16**).** This reaction was conducted analogously to method (a) for **14**, using compound **11** (218.5 mg, 0.44 mmol) in 40 mL of THF and PMePh_2 (89.0 mg, 83.0 μL , 0.44 mmol). Workup was conducted similarly. A cream powder of **16** was obtained in 44.0% yield (120.0 mg, 0.19 mmol) with mp $132\text{--}134\text{ }^{\circ}\text{C}$. IR (KBr): 1613 (s, br), 1587 (w, sh), 1481 (s), 1435 (vs), 1365 (w), 1305 (vs), 1255 (w, sh), 1174 (vs, br), 1110 (s, br), 1050 (vs, br), 899 (vs, br), 848 (w), 814 (vs), 744 (vs, br), 698 (w), 658 (s), 560 (s), 511 (s), 488 (s, sh), 442 (vs). EI-MS (70 eV): m/z , 619 [M^+], 418, 313, 256. Anal. Calcd for $\text{C}_{25}\text{H}_{30}\text{O}_2\text{PSIr}$: C, 48.61; H, 4.89. Found: C, 48.61; H, 5.53.

Synthesis of $[(\eta^4\text{-COD})\text{Ir}(1\text{-}2,5\text{-}\eta\text{-SO}_2\text{CH}=\text{CHCH}=\text{CH}_2)\text{PPh}_3]$ (17**).** (a) This reaction was conducted analogously to that for **14** (a) using compound **11** (100.0 mg, 0.20 mmol) in 10 mL of THF and PPh_3 (53.0 mg, 0.20 mmol). Workup was conducted similarly. A pale cream powder of **17** was obtained in 82.0% yield (113.2 mg, 0.17 mmol), with mp $191\text{--}192\text{ }^{\circ}\text{C}$. Single, yellow-orange crystals were obtained from a CHCl_3 solution at $-40\text{ }^{\circ}\text{C}$. IR (KBr, cm^{-1}): 1617 (w), 1482 (m), 1435 (s), 1307 (m, br), 1188 (vs, sh), 1173 (vs), 1106 (m), 1047 (vs), 816 (s), 754 (m), 733 (w), 659 (m), 618 (w), 558 (m), 525 (s), 466 (w), 442 (m). EI-MS: m/z , 418 [M^+ - L]. Anal.

Calcd for $\text{C}_{30}\text{H}_{32}\text{O}_2\text{PSIr}\cdot\text{CHCl}_3$: C, 46.59; H, 4.16. Found: C, 46.89; H, 4.57.

(b) Compound **22** (100.0 mg, 0.17 mmol) was dissolved in 15 mL of THF to form an orange solution, which was cooled at $-110\text{ }^{\circ}\text{C}$ (liquid N_2/EtOH), and then **3K** (26.1 mg, 0.17 mmol), previously suspended in THF, was added. After addition, the reaction mixture was allowed to reach room temperature and was stirred for 1 h; it gave a yellow solution. The volume of solution was reduced to ~ 3 mL under vacuum; then cold hexane was added to precipitate a cream solid, which was filtered and dried under vacuum; this afforded 60.0 mg (53.0%, 0.09 mmol) of **17**.

Synthesis of $[(\eta^4\text{-COD})\text{Ir}(1\text{-}2,5\text{-}\eta\text{-SO}_2\text{CH}=\text{CHCH}=\text{CH}_2)\text{DMSO}]$ (18**).** (a) A Schlenk was charged with **3K** (47.0 mg, 0.30 mmol) and DMSO (2 mL). After addition of compound **4** (100.0 mg, 0.15 mmol) at room temperature, the reaction mixture was stirred for 1 h; then it was filtered, and the solvent was removed under vacuum using an oil bath at $65\text{--}75\text{ }^{\circ}\text{C}$. An oily residue, along with a pale cream solid, was treated with CH_2Cl_2 . The solution was filtered and evaporated under vacuum, and the powder was washed with hexane. After drying, compound **18** (73.0 mg, 0.15 mmol) was obtained as a pale cream solid in 49.0% yield. Single crystals were obtained from a CHCl_3 solution at room temperature. IR (CHCl_3 , cm^{-1}): 1223 (vs), 1166 (w), 1100 (m), 1051 (vs), 819 (m, br), 781 (m, br), 730 (m, br), 713 (m, br), 661 (m), 563 (w), 446 (m), 416 (s). EI-MS (m/z , %, assignment): 418 [M^+ - L]. Anal. Calcd for $\text{C}_{14}\text{H}_{23}\text{O}_3\text{S}_2\text{Ir}$: C, 33.49; H, 5.09. Found: C, 33.33; H, 5.00.

(b) Compound **11** (100.0 mg, 0.20 mmol) was dissolved in DMSO (3 mL) and stirred, at room temperature, for 1 h. The DMSO was evaporated to dryness under vacuum and an oil bath ($65\text{--}75\text{ }^{\circ}\text{C}$, decomposition of **18** due to the loss of COD was spectroscopically observed at higher temperatures). Extraction with CH_2Cl_2 (30 mL) gave a pale yellow solution, which was filtered, and the volume was reduced to ~ 1 mL; after addition of pentane (20 mL), a pale cream precipitate was obtained. Filtration and drying under vacuum afforded compound **18** in 55.0% yield (55.0 mg, 0.11 mmol). Mp: $152\text{--}153\text{ }^{\circ}\text{C}$ (dec).

Synthesis of $[(\eta^4\text{-COD})\text{Ir}(1\text{-}2,5\text{-}\eta\text{-SO}_2\text{CH}=\text{CHCH}=\text{CH}_2)\text{CO}]$ (19**).** A solution of **11** (100.0 mg, 0.20 mmol) in 15 mL of THF was filtered, at room temperature, to a glass reactor, and CO was introduced at one atmosphere. After stirring 6 min, a precipitate was observed; it was filtered, and column chromatography under silica gel (10×2 cm) with a mixture of solvents THF/ Et_2O (2:1) was carried out. The light brown solution was evaporated until dryness, and a second chromatography (6×2 cm) was carried out with the same mixture of solvents. The light amber solution was evaporated, and 54.0 mg (0.12 mmol) of crystalline, pale amber product **19** was obtained in 60.0% yield, with mp $194\text{--}197\text{ }^{\circ}\text{C}$ (dec). IR (CHCl_3 , νCO , cm^{-1}): 2058 (vs). IR (KBr): 2054 (vs), 1609 (m, br), 1442 (m, br), 1171 (s, br), 1103 (m, br), 1052 (vs, br), 820 (s), 727 (w, br), 697 (w, br), 661 (m, br), 651 (w, br), 528 (m, br), 485 (m, br). Anal. Calcd for $\text{C}_{13}\text{H}_{17}\text{O}_3\text{SiIr}$: C, 35.03; H, 3.85. Found: C, 35.32; H, 4.00.

Synthesis of $[(\eta^4\text{-COD})\text{Ir}(5\text{-}\eta\text{-SO}_2\text{CH}=\text{CHCH}=\text{CH}_2)(\text{PMe}_3)_2]$ (20**).** A solution of **14** (100.0 mg, 0.20 mmol) in 3 mL of benzene was stirred, and PMe_3 (0.13 mL, 1.20 mmol) was added; the mixture was stirred for 1 h at room temperature. The cream powder that precipitated in the reaction mixture was filtered and washed with 3 mL of benzene and dried under vacuum. The very pale cream product **20** was obtained (80.0 mg, 0.14 mmol) in 69.0% yield, with mp $99\text{--}101\text{ }^{\circ}\text{C}$. Single crystals were obtained from slow diffusion of THF/hexane at $-50\text{ }^{\circ}\text{C}$. IR (KBr, cm^{-1}): 1647 (s), 1575 (w, sh), 1477 (w, sh), 1430 (s), 1292 (s), 1163 (vw), 1019 (s, br), 949 (vs, br), 864 (m), 777 (m), 724 (s), 672 (m), 646 (w), 592 (w, br), 465 (w, br). FAB-MS (3-NBA): m/z 569 [M^+].

Synthesis of $[(\eta^4\text{-COD})\text{Ir}(\text{Cl})(\text{PMe}_3)]$ (21**).** Compound $[(\eta^4\text{-COD})\text{Ir}(\mu\text{-Cl})_2]$ (**4**) (200.0 mg, 0.30 mmol) was dissolved in THF (10 mL), giving a red-orange solution, which was treated with PMe_3 (62.0 μL , 0.6 mmol) at $-110\text{ }^{\circ}\text{C}$ (N_2 liquid/ EtOH). The solution turned yellow, the cold bath was removed, and the reaction mixture was allowed to reach room temperature. The solution was filtered, the solvent was removed *in vacuo*, and the residue was washed with

pentane (2 × 10 mL) and dried *in vacuo*. The orange solid (178 mg, 0.43 mmol) was obtained in 73.0% yield and was stored in a refrigerator to avoid decomposition. Mp: 94–96 °C. EI-MS (20 eV): *m/z* 412 [M⁺], 374, 346, 322, 294, 268, 210, 192, 57. IR (KBr, cm⁻¹): 1956 (w, br), 1741 (w, br), 1607 (w, br), 1497 (w), 1469 (m, sh), 1441 (s, sh), 1419 (s), 1326 (m), 1280 (s), 1262 (s), 1159 (w), 1095 (s, br), 1023 (s, br), 954 (vs, br), 880 (s, br), 801 (vs, br), 736 (s), 675 (s), 516 (m), 466 (m). Anal. Calcd for C₁₁H₂₁ClIr: C, 32.07; H, 5.13. Found: C, 32.60; H, 5.28.

Synthesis of [(η⁴-COD)Ir(Cl)(PPh₃)] (22). The synthesis was carried out as described in the literature.^{49,58a} ³¹P NMR and mass spectrometry data are included, because they have not been reported. Crystals were obtained from recrystallization of CH₂Cl₂/hexane at -5 °C. Yield: 86%. Mp: 176–177 °C. EI-MS: *m/z* 598 [M⁺], 560 [M - Cl]⁺, 452 [M - Cl - COD]⁺, 262 [PPh₃]⁺. IR (KBr, cm⁻¹): 1964 (w, br), 1892 (w, br), 1813 (w, br), 1587 (w, br), 1480 (s), 1433 (vs), 1327 (m), 1221 (m), 1183 (m), 1158 (w), 1094 (vs), 1028 (w), 1000 (m), 971 (w), 891 (w), 818 (w), 751 (vs), 697 (vs), 536 (vs), 514 (vs), 493 (vs), 448 (m).

Synthesis of [(η⁴-COD)Ir(Cl)(PMe₃)₂] (23). The synthesis was carried out as described in the literature.⁵⁷ ¹³C and ³¹P NMR, IR spectroscopy, and mass spectrometry data are included because they have not been published. Mp: 112–114 °C (dec). ESI+ TOF: *m/z* 453.1446; error ppm: 0.5044; DBE: 2.0. IR (KBr, cm⁻¹): 1960 (w, br), 1656 (w, sh), 1623 (m), 1479 (w, sh), 1432 (s), 1293 (s), 1257 (w), 1211 (w), 1187 (w), 1164 (w), 1045 (w), 973 (vs, sh), 953 (vs, br), 868 (s), 725 (s), 673 (s), 466 (w).

Synthesis of [(η⁴-COD)Ir(PMe₃)₃]Cl (24). The synthesis was carried out as described in the literature.⁵⁹ ¹³C and ³¹P NMR, IR spectroscopy, and mass spectrometry data and chemical analysis are included. Mp: 140–141 °C (dec). ESI+ TOF: *m/z* 529.1891; error ppm: 0.4531; DBE: 1.0. IR (KBr, cm⁻¹): 1623 (m), 1479 (vw, sh), 1432 (s), 1325 (vw, sh), 1293 (s), 1244 (w), 1210 (w), 1187 (w), 1164 (w), 1044 (w), 976 (vs, sh), 953 (vs, br), 902 (s, sh), 868 (s), 793 (vw), 725 (s), 673 (s), 466 (w). ¹H NMR (CDCl₃, 300 MHz): δ 1.63 (m, 3H), 2.24 (m, 4H), 2.38 (m, 4H), 3.22 (m, 4H). ¹³C{¹H} NMR (CDCl₃, 75.5 MHz): δ 20.0 (m, PMe₃), 34.1 (s, CH₂COD), 68.5 (m, J = 4.8 Hz, CH, COD). ³¹P NMR (CDCl₃, 121.5 MHz): -52.35 (s). Anal. Calcd for C₁₇H₃₉ClP₃Ir: C, 36.20; H, 6.97. Found: C, 36.22; H, 6.87.

Reactivity of Compound 8 in CDCl₃. Compound 8 (16.0 mg, 0.02 mmol) was dissolved in CDCl₃ (0.5 mL) and then transferred to a NMR sealed tube. After 22 days at room temperature, 8 was almost consumed, and the ¹H and ³¹P NMR spectra were in agreement with the formation of the tentative complex [Ir(η-CH₂CHCHSO₂)-CO(PPh₃)₂]. The ¹H NMR showed chemical shifts at 4.85 (dd, J = 17.0, 1.8, H1); 4.73 (d, J = 10.3, H2); 6.46 (m, H3); 5.51 (dd, J = 10.1, 10.1, H4); 5.66 (d, J = 9.2, H5), and ³¹P NMR showed a singlet at 2.33 ppm.

Reaction of 12 and 3K. Mixture of Compounds (η⁴-COD)Ir(1-2,5-η-CH₂=CHCH=CHSO₂)(5-η-S(O₂⁻K⁺)CH=CH=CH₂) (13), 3K, and 11. Compound 12 (150.0 mg, 0.20 mmol) and 3K (93.0 mg, 0.60 mmol) were dissolved in THF (25 mL) and stirred at room temperature for 1 h. The pale yellow turbid solution was filtered to afford 3K, and the volume of the filtered solution was reduced to 5 mL under vacuum. After addition of pentane (60 mL) a cream solid was precipitated and filtered to afford, according to ¹H NMR (DMSO-d₆), a mixture of compounds 13 and 11 in 3:1 ratio.

Identification of the Mixture of Compounds 14, 20, and 20′. NMR tubes containing compound 12 (40.0 mg, 0.05 mmol) or 11 (60.0 mg, 0.12 mmol) and 0.8 mL of C₆D₆O were prepared. PMe₃ was added, at room temperature, into each NMR tube at 6.0 μL (0.05 mmol) or 13.0 μL (0.12 mmol), respectively. Consecutive addition of PMe₃ occurred until three equivalents gave evidence of the equilibrium among 14, 20, and 20′. In the former, two equivalents of 3K were then added, followed by three more equivalents of PMe₃, giving spectroscopic evidence of the equilibrium described above.

An NMR tube containing compound 14 (60.0 mg, 0.12 mmol) and 0.8 mL of C₆D₆ was prepared. Addition of three subsequent

equivalents of PMe₃ (3 × 13.0 μL, 3 × 0.12 mmol), at room temperature, afforded a mixture of compounds 14, 20, and 20′.

■ ASSOCIATED CONTENT

📄 Supporting Information

Tables of crystallographic data, including atomic coordinates, bond lengths and angles, anisotropic thermal parameters, and least-squares planes for compounds 5, 9, 12, 14, 15, 17–20 (CCDC 840745–840753) and 22. IR spectra of compound 11, ¹H and ¹³C NMR of compounds 5, 12, and 19, as well as ³¹P NMR spectra of monitoring reactions of 11 with PMe₃ and 12 with PMe₃ and 3K. Spectroscopic evidence of the transformation of 8 in CDCl₃ and voltammograms of the electrochemistry experiments of 11 and 18; experimental evidence in solution and in the solid state of KCl, as well as DLS size distribution of 10, 11, and 17 and TGA of compound 11. This material is available free of charge via the Internet at <http://pubs.acs.org>.

■ AUTHOR INFORMATION

Corresponding Author

*E-mail: mpaz@cinvestav.mx.

■ ACKNOWLEDGMENTS

Financial support for this work was provided by Conacyt, Mexico (46556-E). P.G.M., B.P.M., and N.P.M.N. thank Conacyt for graduate and undergraduated scholarships. We thank P. Juárez-Saavedra, V. M. González Diaz, G. Cuellar Rivera, M. A. Leyva Ramirez, and M. Campos for assistance with some of the IR and microanalysis, NMR, mass spectra, X-ray diffraction studies, and TGA analysis, respectively. The authors would also like to thank an anonymous reviewer for insightful suggestions.

■ REFERENCES

- (1) (a) Powell, P. *Adv. Organomet. Chem.* **1986**, *26*, 125. (b) Ernst, R. D. *Chem. Rev.* **1988**, *88*, 1255. (c) Ernst, R. D. *Comments Inorg. Chem.* **1999**, *21*, 285. (d) Yasuda, H.; Nakamura, A. *J. Organomet. Chem.* **1985**, *285*, 15.
- (2) Bleeke, J. R.; Ortwerth, M. F.; Rohde, A. M. *Organometallics* **1995**, *14*, 2813.
- (3) Bleeke, J. R.; Hinkle, P. V.; Rath, N. P. *Organometallics* **2001**, *20*, 1939.
- (4) Bleeke, J. R.; Ortwerth, M. F.; Chiang, M. Y. *Organometallics* **1992**, *11*, 2740.
- (5) Bleeke, J. R.; Ortwerth, M. F.; Chiang, M. Y. *Organometallics* **1993**, *12*, 985.
- (6) (a) Bleeke, J. R.; Hinkle, P. V.; Rath, N. P. *J. Am. Chem. Soc.* **1999**, *121*, 595. (b) Bleeke, J. R. *Chem. Rev.* **2001**, *101*, 1205.
- (7) Hachgenei, J. W.; Angelici, R. J. *J. Organomet. Chem.* **1988**, *355*, 359.
- (8) Spies, G. H.; Angelici, R. J. *Organometallics* **1987**, *6*, 1897.
- (9) Hachgenei, J. W.; Angelici, R. J. *Angew. Chem., Int. Ed. Engl.* **1987**, *26*, 909.
- (10) Bleeke, J. R. *Organometallics* **2005**, *24*, 5190.
- (11) Bianchini, C.; Meli, A.; Peruzzini, M.; Vizza, F.; Fedriani, P.; Herrera, V.; Sanchez-Delgado, R. *J. Am. Chem. Soc.* **1993**, *115*, 2731.
- (12) Paz-Sandoval, M. A.; Cervantes-Vasquez, M.; Young, V. G. Jr.; Guzei, I. A.; Angelici, R. J. *Organometallics* **2004**, *23*, 1274.
- (13) Chen, J.; Su, Y.; Jacobson, R. A.; Angelici, R. J. *J. Organomet. Chem.* **1996**, *512*, 149.
- (14) Paz-Sandoval, M. A.; Cervantes-Vasquez, M.; Paz-Michel, B. *ARKIVOC* **2008**, *v*, 124.
- (15) Gamero-Melo, P.; Sanchez-Castro, M. E.; Ramirez-Moroy, A.; Paz-Sandoval, M. A. *Organometallics* **2004**, *23*, 3290.

- (16) Paz-Michel, B.; Cervantes-Vasquez, M.; Paz-Sandoval, M. A. *Inorg. Chim. Acta* **2008**, *361*, 3094.
- (17) Gamero-Melo, P. Dissertation, *Cinvestav*, 2004.
- (18) Paz-Michel, B. Dissertation, *Cinvestav*, 2009.
- (19) Gamero-Melo, P.; Villanueva-Garcia, M.; Robles, J.; Contreras, R.; Paz-Sandoval, M. A. *J. Organomet. Chem.* **2005**, *690*, 1379.
- (20) Paz-Sandoval, M. A.; Rangel-Salas, I. I. *Coord. Chem. Rev.* **2006**, *250*, 1071.
- (21) Takagi, F.; Seino, H.; Mizobe, Y.; Hidai, M. *Organometallics* **2002**, *21*, 694.
- (22) (a) Tang, Z.; Nomura, Y.; Ishii, Y.; Mizobe, Y.; Hidai, M. *Inorg. Chim. Acta* **1998**, *267*, 73. (b) Hashizume, K.; Mizobe, Y.; Hidai, M. *Organometallics* **1996**, *15*, 3303, and references therein.
- (23) Angelici, R. J. *Organometallics* **2001**, *20*, 1259.
- (24) Chisholm, M., Ed. Modeling the Chemistry of Hydrotreating Processes. *Polyhedron* **1997**, *16*, 3071.
- (25) Bianchini, C.; Meli, A.; Peruzzini, M.; Vizza, F.; Moneti, S.; Herrera, V.; Sanchez-Delgado, R. A. *J. Am. Chem. Soc.* **1994**, *116*, 4370.
- (26) Bianchini, C.; Jimenez, M. V.; Meli, A.; Moneti, S.; Vizza, F. *J. Organomet. Chem.* **1995**, *504*, 27.
- (27) Bianchini, C.; Casares, J. A.; Masi, D.; Meli, A.; Pohl, F.; Vizza, F. *J. Organomet. Chem.* **1997**, *541*, 143.
- (28) (a) Bianchini, C.; Jimenez, M. V.; Meli, A.; Vizza, F. *Organometallics* **1995**, *14*, 3196. (b) Bianchini, C.; Jimenez, M. V.; Meli, A.; Vizza, F. *Organometallics* **1995**, *14*, 4858.
- (29) Bianchini, C.; Frediani, P.; Herrera, V.; Jimenez, M. V.; Meli, A.; Rincon, L.; Sanchez-Delgado, R. A.; Vizza, F. *J. Am. Chem. Soc.* **1995**, *117*, 4333.
- (30) (a) Bleeke, J. R.; Wise, E. S.; Shokeen, M. *Organometallics* **2005**, *24*, 805. (b) Bleeke, J. R.; Shokeen, M.; Wise, E. S. *Organometallics* **2006**, *25*, 2486.
- (31) Bleeke, J. R.; Boorsma, D.; Chiang, M. Y.; Clayton, T. W. Jr.; Haile, T.; Beatty, A. M.; Xie, Y.-F. *Organometallics* **1991**, *10*, 2391.
- (32) A 16-electron complex $[\text{Ir}(\eta^5\text{-CH}_2\text{CHCHCHS})(\text{CO})(\text{PPh}_3)_2]_n$ ($n = 1$) may be proposed, according to the presence of the bulky phosphines and results observed in complex $(\eta^4\text{-COD})\text{Ir}(\eta^5\text{-CH}_2\text{CHCHCHSO}_2)(\text{PMe}_3)_2$ (**20**). However, a dimeric 18-electron compound ($n = 2$) could not be ruled out, because the mirror-plane in the molecule makes the two PPh_3 ligands equivalent.
- (33) Calligaris, M. *Croatia Chem. Acta* **1999**, *72* (2–3), 147.
- (34) Paz-Michel, B.; Gonzalez-Bravo, F. J.; Hernandez-Muñoz, L. S.; Guzei, I. A.; Paz-Sandoval, M. A. *Organometallics* **2010**, *29*, 3694.
- (35) Paz-Michel, B.; Gonzalez-Bravo, F. J.; Hernandez-Muñoz, L. S.; Paz-Sandoval, M. A. *Organometallics* **2010**, *29*, 3709.
- (36) Vitzthum, G.; Lindner, E. *Angew. Chem., Int. Ed. Engl.* **1971**, *10*, 315.
- (37) Cotton, F. A.; Lahuerta, P.; Sanau, M.; Schwotzer, W. *Inorg. Chim. Acta* **1986**, *120*, 153.
- (38) Although unambiguous characterization of **20'** was not possible, we base the formulation on ^1H and ^{13}C NMR spectra from the mixture of reaction with **14** and **20**, obtained from reaction of **14** with consecutive addition of PMe_3 in C_6D_6 ; see text. The tentative assignment of $[(\eta^4\text{-COD})\text{Ir}(\eta^5\text{-SO}_2\text{CHCHCHCH}_2)(\text{PMe}_3)_2]$ (**20'**): ^1H NMR (C_6D_6): δ 5.10 (d, 6.6, H1), 5.13 (d, 10.8, 17.4, H1'), 8.51 (dt, 6.5, 17.2, H2), 5.79 (t, 10.8, H3), 6.55 (d, 11.1, H4), 1.33 (d, 7.9, PMe_3), 3.26 (s, br, CH, COD), 1.88–2.30 (m, CH_2 , COD). $^{13}\text{C}\{^1\text{H}\}$ NMR (C_6D_6): δ 120.2 (C1), 133.3 (C2), 127.8 (C3), 145.4 (t, 3.1, C4), 67.6 (t, 4.6, 5.4, CH_2 , COD), 33.9 (CH_2 , COD), 18.3 (m, 3.8, 33.1, PMe_3). ^{31}P NMR (C_6D_6): δ -46.22 (s).
- (39) Compounds **23** and **24** could not be excluded from the reaction mixture, because both could not be discriminated from **20** by ^1H , ^{13}C , and ^{31}P NMR data. See Tables 3 and 4. Compound **20** can only be recognized in the ^1H and ^{13}C NMR through the corresponding chemical shifts of the butadienesulfonyl ligand.
- (40) Jesse, A. C.; van Baar, J. F.; Stufkens, D. J.; Vrieze, K. *Inorg. Chim. Acta* **1976**, *17*, L13.
- (41) Prestbo, E. W.; Melethil, P. K.; McHale, J. L. *J. Phys. Chem.* **1983**, *87*, 3883.
- (42) Fawcett, W. R.; Kloss, A. A. *J. Phys. Chem.* **1996**, *100*, 2019.
- (43) Randall, S. L.; Miller, C. A.; Janik, T. S.; Churchill, M. R.; Atwood, J. D. *Organometallics* **1994**, *13*, 141.
- (44) Vaska, L.; Bath, S. S. *J. Am. Chem. Soc.* **1966**, *88*, 1333.
- (45) Abernethy, R. J.; Hill, A. F.; Tshabang, N.; Willis, A. C.; Young, R. D. *Organometallics* **2009**, *28*, 488.
- (46) Serli, B.; Zangrando, E.; Gianferrara, T.; Yellowless, L.; Alessio, E. *Coord. Chem. Rev.* **2003**, *245*, 73.
- (47) Sunley, G. J.; Menanteau, P. C.; Adams, H.; Bailey, N. A.; Maitlis, P. M. *J. Chem. Soc., Dalton Trans.* **1989**, 2415.
- (48) Gomez, M.; Yarrow, P. I. W.; Vazquez de Miguel, A.; Maitlis, P. M. *J. Organomet. Chem.* **1983**, *259*, 237.
- (49) Crabtree, R. H.; Morris, G. J. *Organomet. Chem.* **1977**, *135*, 395.
- (50) Huheey, J. E.; Keiter, E. A.; Keiter, R. L. *Inorganic Chemistry*, 4th ed.; Harper & Row: New York, 1993; Appendix E (A-30) and references therein.
- (51) (a) Ryan, R. R.; Kubas, G. J.; Moody, D. C.; Eller, P. G. *Struct. Bonding* **1981**, *46*, 47.
- (52) (a) Hettler, D. G. H.; Klop, M.; Kicken, R. J. N. A. M.; Smits, J. M. M.; Reijerse, E. J.; de Bruin, B. *Chem.—Eur. J.* **2007**, *13*, 3386. (b) Rossi, A. R.; Hoffmann, R. *Inorg. Chem.* **1975**, *14*, 365.
- (53) Lebel, H.; Ladjel, C. *Organometallics* **2008**, *27*, 2676, and references therein..
- (54) Lefort, L.; Lachicotte, R. J.; Jones, W. D. *Organometallics* **1998**, *17*, 1420.
- (55) Herde, J. L.; Lambert, J. C.; Senoff, C. V. *Inorg. Synth.* **1982**, *15*, 18.
- (56) Vrieze, K.; Collman, J. P.; Sears, C. T. Jr.; Kubota, M. *Inorg. Synth* **1978**, *11*, 101.
- (57) Burk, M.; Crabtree, R. *Inorg. Chem.* **1986**, *25*, 931.
- (58) (a) Winkhaus, G.; Singer, H. *Chem. Ber.* **1966**, *99*, 3610. (b) Vrieze, K.; Volger, H.; Praat, A. P. *J. Organomet. Chem.* **1968**, *14*, 185. (c) Denise, B.; Pannetier, G. *J. Organomet. Chem.* **1975**, *99*, 455. (d) Denise, B.; Pannetier, G. *J. Organomet. Chem.* **1978**, *148*, 155. (e) De Aquino, W.; Bonnaire, R.; Potvin, C. *J. Organomet. Chem.* **1978**, *154*, 159. (f) Volger, H.; Vrieze, K.; Praat, A. P. *J. Organomet. Chem.* **1968**, *14*, 429. (g) Haszeldine, R. N.; Lunt, R. J.; Parish, R. V. *J. Chem. Soc. (A)* **1971**, 3711.
- (59) (a) Merola, J. S.; Kacmarcik, R. T. *Organometallics* **1989**, *8*, 778. (b) Frazier, J. F.; Merola, J. S. *Polyhedron* **1992**, *11*, 2917.